VentoFoil Adoption Model

A computational modelling approach on the financial and environmental impact of VentoFoil placement on a vessel

MSc Marine Technology Thesis - Report

Mo Smeets

TU Delft

ECONOWIND

This page is left blank intentionally.

Thesis for the degree of MSc in Marine Technology in the specialization of Ship Design

VentoFoil Adoption Model

A computational modelling approach on the financial and environmental impact of VentoFoil placement on a vessel

By

Mo Smeets

Performed at

Econowind

29-11-2024

Company supervisor
Responsible and daily supervisor: Ir. Rens Groot

Thesis exam committee
Chair/Responsible Professor: Dr. Austin Kana
Staff Member: Ir. Jaap Gelling
Staff Member: Dr. Ir. Albert Rijkens
Company Member: Ir. Rens Groot

Author Details
Studynumber: 4835018

Cover: Chemship BV, 2024

TU Delft ECONOWIND

Contents

Preface

This report was written as part of my master's thesis on the VentoFoil Adoption Model. Within this thesis period, a VentoFoil Adoption Model was constructed to support shipowners in making informed decisions on whether and where to place VentoFoils on board. As a sailor interested in sustainable solutions onboard cargo vessels, Econowind and its VentoFoils were the ideal way to combine my interest in this project. I am pleased by the enthusiasm at Econowind about the model and excited to see it put to use in their projects.

I want to express my thanks to Austin and Rens, my daily supervisors during this thesis, for guiding me in the right direction and providing valuable feedback throughout the process. I am also grateful to my friends and family around me for their support. I particularly appreciated the experience of working alongside friends as we each worked on our own theses. Special thanks to Marijn, for assisting me with programming issues and keeping me motivated.

During this final phase of my study career, I have learned a lot about programming, ship design, maritime decision-making, and independently managing my own project. I look forward to working on sustainable maritime transport solutions.

This thesis is intended for researchers, students, and professionals working on sustainable solutions in the field of maritime technology. I hope that it provides valuable insights and contributes to the ongoing conversation around the adoption of wind-assisted propulsion systems.

Mo Smeets
Delft, November 2024

Summary

For centuries, sailing was the main way of transporting cargo overseas. However, with the invention of the steam engine, this became the main propulsor since it was more efficient and redundant. Due to more awareness of the effect of greenhouse gases on the environment and therefore IMO regulations on emissions, Wind Assisted Propulsion Systems have become more and more interesting for shipowners. One of those Wind Assisted Propulsion Systems is the VentoFoil from Econowind. However, to enable the decision of the shipowner on whether and where to place VentoFoils on board, this research aimed to construct a VentoFoil Adoption model, assessing the environmental and financial consequences of specific VentoFoil placement options. With this, the main research question is: 'What is the impact of VentoFoil placement on ships from a ship owner's perspective?' The VentoFoil Adoption Model for Econowind required a Technology Adoption Decision-support model that could operate within a short computational time while incorporating an adaptable weather matrix. During the literature study on the existing models regarding WASP models, a research gap was identified. The gap primarily lies in integrating low-fidelity force modelling with financial decision support.

The VentoFoil Adoption model was constructed with a baseline calculation in which no VentoFoils were placed onboard. This baseline included the hull resistance and the wind forces on the deckhouse for all possible wind directions and speeds. After that, the VentoFoils were placed on deck, for which the VentoFoil forces were added with respect to the baseline calculations. The VentoFoil forces were calculated including the interaction between the deck and the VentoFoils, using a turbulent separation layer. The interaction between the deckhouse and the VentoFoils was simulated using a triangle shape in which the wake is turbulent. Lastly, the interaction between the VentoFoils was included using a parametrized wakefield in which the apparent wind angle changed based on the distance between the VentoFoils. The output of the model includes the polar plot. In the model, the VentoFoil is divided into height elements making it possible to make use of the wind gradient and to specify which height element would have interacting effects. From the resulting polar plots, the financial and environmental benefits of VentoFoils are illustrated. Fuel savings are achieved when sailing at reference speed and lower power, and increased cargo yield is realized at higher speeds with reference power. This is dependent on the weather probability matrix. The EEXI benefits are calculated based on the ideal polar plot since IMO does not demand the EEXI calculation on realistic polar plots yet.

To demonstrate the practical application and effectiveness of the model, a case study was performed using the VentoFoil Adoption Model on the Magritte, a bulk carrier currently sailing with two 16-meter VentoFoils. The goal was to find trends in VentoFoil placement and to compare the possible placement options from different perspectives. From a shipowner's perspective, the conclusion was made that two 30-meter VentoFoils would in the long term be more cost-effective. However, this depends on the fuel price, cargo yield and sailing speed. For most combinations of fuel price and cargo yield, the payback time of the case at reference power and thus higher sailing speed was lower, making it the favourable operational decision. The change in sailing speed, in contrast, is not very high, raising the question of whether this is indeed noticeable in the cargo yield increase.

A validation using the 'validation square method' was performed on the method used within the VentoFoil Adoption Model. One of the four squares is the empirical performance validity, which was investigated by comparing the results from sea trial data of the MV Sunnanvik and results from the model. The results at reference speed were a bit conservative although the results at reference power were a bit optimistic. The results are within a reasonable range.

The answer to the main research question can be found with the model. Multiple placement options can be inserted, giving the benefits and costs for well-considered decision-making of the ship owner on whether and where to place VentoFoils on board.

Nomenclature

Abbreviations

Abbreviation	Definition
ABM	Agent-based modelling
AI	Artificial Intelligence
CFD	Computational Fluid Dynamics
CoE	Centre of Effort
CoG	Centre of Gravity
CO_2	Carbon Dioxide
CII	Carbon Intensity Indicator
DNV	Det Norske Veritas (Class agency)
DOF	Degree(s) of freedom
EARSM	Explicit Algebraic Reynolds Stress Model
EEDI	Energy Efficiency Design Index
EEXI	Energy Efficiency Existing Ships Index
EMSA	European Maritime Safety Agency
FPP	Fuel Prediction Program
GHG	Greenhouse gas
GUI	Graphical user interface
HFO	Heavy fuel oil
IMO	International Maritime Organisation
LCG	Longitudinal Centre of Gravity
LL	Lifting Line
NACA	National Advisory Committee for Aeronautics
MCR	Maximum Continuous Rating
PPP	Performance Prediction Program
PPPS	Pelican Performance Prediction Software
RANS	Reynolds Averaged Navier-Stokes
RQ	Requirement
RW	Rigid Wing
SST	Shear Stress Transport
SRANS	Steady Reynolds-Averaged Navier-Stokes
TF	Trailing edge plain flap
URANS	Unsteady Reynolds Averaged Navier-Stokes
VCG	Vertical Centre of Gravity
VLCC	Very Large Crude Carrier
VPP	Velocity Prediction Program
WAPS	Wind-Assisted Propulsion System (only the system)
WASP	Wind-Assisted Ship Propulsion (ship with integrated system)
WPT	Wind Propulsion Technology

Symbols

Symbol	Definition	Unit
A	Surface	[m^2]
AR	Aspect Ratio Rotor (height / diameter)	[-]
AoA	Angle of Attack	[°]
$A_{projected}$	Projected area	[m^2]
AWA	Apparent Wind Angle	[°]
AWS	Apparent Wind Speed	[m/s]
B_n	Parameterized width of the VentoFoil placement	[m]
b	Breadth of the column in the strength calculations	[m]
C_D	Drag coefficient	[-]
C_E	Resistance coefficient	[-]
C_L	Lift coefficient	[-]
C_q	Suction coefficient	[-]
C_{TF}/C_{RW}	Flap chord ratio Rigid Wing Sails	[-]
C_X	Thrust coefficient	[-]
CY	Cargo yield	[$]
c	Cord length	[m]
c_1	Resistance coefficient	[-]
d	Coordinate system in line with the Drag	[-]
D	Drag	[kN]
D	Bending stiffness of the plate in the strength calculations	[GPa·m^3]
De/D	Endplate size factor Rotor (diameter endplate / diameter rotor)	[-]
D_R	Relative distance between VentiFoils	[m]
DWT	Deadweight	[MT]
d_{TF}	Flap deflection Rigid Wing Sails	[°]
E	Elasticity modulus	[GPa]
EX	Expected value (probability)	[unit of X]
f_{wind}	Reward factor wind-assisted vessels FuelEU Maritime	[-]
F	Force	[kN]
FC	Fuel consumption	[ton]
FR	Freight rate	[$]
F_{WAPS}	WAPS Force (in the x-direction)	[kN]
F_x	Force in longitudinal direction	[kN]
h	Height (Altitude) of the wind speed	[m]
h	Thickness of the plates within a column in the strength calculations	[m]
I	Moment of inertia	[m^4]
k'	Cross flow drag coefficient	[-]
k_c	Buckling coefficient	[-]
l	Coordinate system in line with the Lift	[-]
l	Length of a beam in strength calculations	[m]
L	Lift	[kN]
$L_{betweenfoils}$	Distance between two interacting VentoFoils	[m]
$L_{influenced}$	Length of the influenced zone	[m]
L_n	Parameterized length of the VentoFoil placement	[m]
M	Moment	[N/m]
m	Buckling mode	[-]
P	Power	[kW]
$(P_{cr})_{column}$	Critical force of the column	[kN]
$(P_{cr})_{plate}$	Critical force of the plate within a column	[kN]

Symbol	Definition	Unit
P_B	Engine Brake Power	[kW]
P_{Bref}	Engine Brake Power in normal operation	[kW]
P_E	Total Effective Power of the vessel	[kW]
$P_{E,engine}$	Effective Power of the engine	[kW]
$P_{E,vento}$	Effective Power of the VentoFoils	[kW]
P_p	Propulsive power	[kW]
P_{fan}	Power of the fan	[kW]
P_{rated}	Rated Power of the fan per area	[kW/m^2]
P_{wind}	Wind power	[kW]
p	Pressure	[Pa]
R_A	Air resistance	[kN]
$Re_{x_{sep}}$	The Reynolds number of the wind at the VentoFoil	[-]
R_F	Skin Friction Drag	[kN]
R_T	Total resistance	[kN]
sfc	Specific fuel consumption	[ton/kWh]
s	Number of stiffeners on one plate in the strength calculation	[-]
t	Thrust deduction factor	[-]
T	Thrust force	[kN]
T/C	Thickness-to-chord ratio	[-]
$t_{sailed/year}$	Time sailed per year	[days]
TtW	Tank-to-wake	[CO_{2eq}]
TWS	True Wind Speed	[m/s]
U	Tangential Velocity of the ship (in y-direction)	[m/s]
U_a	Apparent wind velocity	[m/s]
$U_{a,inter}$	Apparent wind velocity at the interacting VentoFoil	[m/s]
$U_{a,\infty}$	Apparent wind velocity at the far-field	[m/s]
U_{min}	Minimum wind speed for the fan to be turned on	[m/s]
U_{max}	Max wind speed for the fan to be turned on	[m/s]
U_{rated}	Rated wind speed for the fan to start blowing at P_{rated}	[m/s]
$P_x(x_k)$	Probability of value x_k	[-]
U_t	True wind velocity	[m/s]
$Var(X)$	Variance	[unit of X]
V_a	Apparent wind speed	[m/s]
V_{ref}	Velocity of the ship in normal operation	[m/s]
V_s	Velocity of the ship (in x-direction)	[m/s]
V_w	Velocity of the wind	[m/s]
v_{10m}	Wind speed at a height of 10 m for the wind gradient	[m/s]
$v_{z_{ref}}$	Wind speed at height z_{ref} for the wind gradient	[m/s]
$W_{i,j}$	Wind probability for different wind speeds and angles	[-]
WtT	Well-to-tank	[CO_{2eq}]
x_{sep}	Distance between the first touch of the deck till the VentoFoil	[m]
x_k	Value with a certain probability	[unit of X]
z_{ref}	Reference height for the wind gradient	[m]
α	Hellman exponent	[-]
α_e	Effective angle of attack	[deg]
α_∞	Undisturbed angle of attack	[deg]
η_D	Total efficiency of the main drive(s) at 75% MCR	[-]
β_a	Apparent wind angle	[deg]
$\beta_{a,inter}$	Apparent wind angle at the interacting VentoFoil	[deg]
β_t	True wind angle	[deg]

Symbol	Definition	Unit
Δ	Displacement	[ton]
δ_{lam}	Height of the laminar part of the separation layer	[m]
δ_{turb}	Height of the turbulent part of the separation layer	[m]
μ_{air}	Dynamic viscosity of air	[Pa· s]
ν	Poisson's ratio	[-]
ρ	Density (seawater/air)	[kg/m^3]
σ	Standard deviation	[unit of X]
$(\sigma_{cr})_{column}$	Critical stress of the column in the strength calculations	[Pa]
$(\sigma_{cr})_{plate}$	Critical stress of the plate within the column in the strength calculations	[Pa]

AI Acknowledgments

During the preparation of this work, I used ChatGPT and Grammarly to check grammar and spelling and to assist in fixing programming errors. Next to that, I used Perplexity to check my understanding of certain papers. After using this tool/service, the author reviewed and edited the content as needed and takes full responsibility for the content of the publication.

1 Introduction

As a consequence of the International Maritime Organisation's (IMO) regulations of 2018, the maritime industry has gained interest in wind-assisted ship propulsion (WASP), as a way to reduce their emissions (Chou et al., 2021). To meet the demand, several companies started developing Wind-Assisted Propulsion Systems (WAPS). In this report Wind Assisted Ship Propulsion, 'WASP' is used for the integration between the vessel and Wind-Assist system and 'WAPS' is the system as a separate unit. One of those systems is the VentoFoil from Econowind (figure 1.1). It is a suction wing, with its working principle and developments described in more detail in section 2.1.

Figure 1.1: VentoFoil placed on a tanker (Chemship BV, 2024)

To make an informed decision about whether to adopt a WAPS, it's crucial to calculate the force balance of the vessel equipped with a WAPS. From this, an estimation of the power and fuel consumption of the systems can be calculated. With these calculation methods, different routes, placements, numbers of WAPSs, and sailing speeds can be compared. A comparison between WAPSs is only possible if the system's impact on costs and emissions is determined. There are several models, specialized in for example force balancing or routing. However, a complete model including the financial and environmental impact of a WAPS, specifically VentoFoils, is still missing.

Within this master's thesis, the focus will be on creating such a complete model. A holistic model to decide as a shipowner whether to install VentoFoils, based on the financial and environmental impact of VentoFoil placement. This decision depends on different placements of the VentoFoils and the change in ship speed, deadweight, and/or power.

This report is structured based on the subquestions of this research, which are described below. In chapter 2, the current status of VentoFoils research and development is explained, followed by the requirements for a VentoFoil Adoption Model. Chapter 3 dives into the existing wind-assisted propulsion system models and ends with an analysis of what requirements are met. After that, it is explained how the model is constructed in chapter 4. A case study on the placement options on an existing vessel assists in answering subquestions 4 and 5 in chapter 5. In chapter 6, the validation of the model is described using the Validity square method. Finally, the conclusion and the discussion reflect on the research and the results in chapters 7 and 8 respectively.

1.1. Research questions

To build a VentoFoil adoption decision-support model the following research questions are formulated, with the goal of answering the main research question, being the following:

'What is the impact of VentoFoil placement on ships from a ship owner's perspective?'

To reach the objective of building a VentoFoil Adoption decision-support model and answer the main research question, the following sub-questions have been composed:

SQ1: What is the current status of VentoFoils research and development, and what requirements must be met for a model assessing their adoption and impact on the vessel's finances and emissions? (Chapter 2)

SQ2: What existing models of wind-assisted propulsion are available, and what are the underlying mechanisms of each? (Chapter 3)

SQ3: How can an early-stage VentoFoil adoption decision-support model be developed to model the force balance of VentoFoil placement on a vessel under varying weather conditions, and assess their financial and environmental benefits? (Chapter 4)

SQ4: How do wind-assisting VentoFoils, or suction wings in general, influence the sailing speed, deadweight, and/or propulsion power of the vessel? (Chapter 5)

SQ5: What financial and environmental trends can be identified through the computational model for vessels equipped with VentoFoils for the different operational profiles? (Chapter 5)

SQ6: How can the predictions of the computational model regarding the influence of VentoFoils on a vessel be validated? (Chapter 6)

2

VentoFoils and Model Requirements

This chapter answers the first subquestion: *SQ1: What is the current status of VentoFoils research and development, and what requirements must be met for a model assessing their adoption and impact on the vessel's finances and emissions?* At first, the VentoFoil working principle will be described in section 2.1, together with the developments and research performed on VentiFoils. Then, the different types and sizes of VentoFoils are described in section 2.2. The requirements for a model assessing VentoFoil adoption will be described (section 2.3). Lastly, the answer to SQ1 will be given in the conclusion in section 2.4.

2.1. VentoFoil working principle

In 1985, Cousteau investigated multiple shapes of 'turbo sails', orientable aspirated cylinders as they were called at the time. The suction wings, as we call them today, have a relatively high thickness-to-cord ratio (T/C-ratio) and a partly porous skin through which boundary layer suction is applied with fans. This boundary layer suction results in a higher lift coefficient (C_L) as is shown for the specific shape 'Moulin à Vent I' in figure 2.1, where the lift coefficient is plotted over the angle of attack. The lift coefficient increases for increasing suction coefficients (C_q) with a maximum of approximately 8.5 (Cousteau et al., 1985). NACA profiles are standardized wing shapes, which are widely used in aircraft design. The highest lift coefficient of a NACA profile is 1.78 for reference (NACA-23012) (Vigna and Figari, 2023).

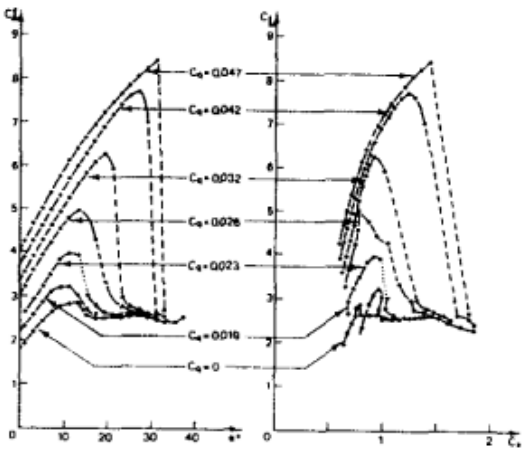

Figure 2.1: Moulin à Vent I results plotted as C_L over α (left) and C_L over C_D (right) (Cousteau et al., 1985)

The shapes Cousteau investigated are similar to the first VentiFoils from Econowind. The working principle of the VentiFoil is shown in figure 2.2a. On both sides of the foil, there are holes where suction is applied. A moving flap covers the holes on the lee side of the wing. Fans are installed at the top and bottom of the VentiFoil for the suction. Tacking is done by switching the flap to the other side. The disadvantage of this system is the moving flap, which is relatively difficult to build and high in maintenance. The suction differs along the height of the foil, with the greatest suction occurring at the top and bottom due to the placement of the fans. The studies performed on VentiFoils are described in section 3.1.5 and 3.1.6.

Econowind developed the VentoFoil as the successor of the VentiFoil, which is optimized for scaling purposes. The working principle of the VentoFoil is shown in figure 2.2. The moving flap of the VentiFoil is replaced by a longer fixed flap. Lagendijk (2018) performed CFD for a moving flap and different

sizes of flaps. From that, the best result was the VentiFoil with the flap at the biggest angle and the longest flap. Although he did not investigate a long flap at the center, this now seems to be the most effective way for a suction wing. An advantage of a fixed flap is the easier production and reduction in maintenance costs. The fixed flap has holes for suction on both sides which are always open. The fans are placed vertically at multiple heights pumping from the leeward side to the luff side. Tacking is done by changing the direction of the fans and changing the angle of attack to the other side. In the CFD analysis in figure 2.3, the effect on the luff side of the VentoFoil can be seen as turbulence due to the van blowing air out on that side.

Another adjustment that was made with the VentoFoil is the addition of an endplate on top of the foil. This endplate reduces the tip vortex, making the wing-shape more efficient in 3D (Gehlert et al., 2021). This is not shown in figure 2.2b, but can be seen in figure 1.1.

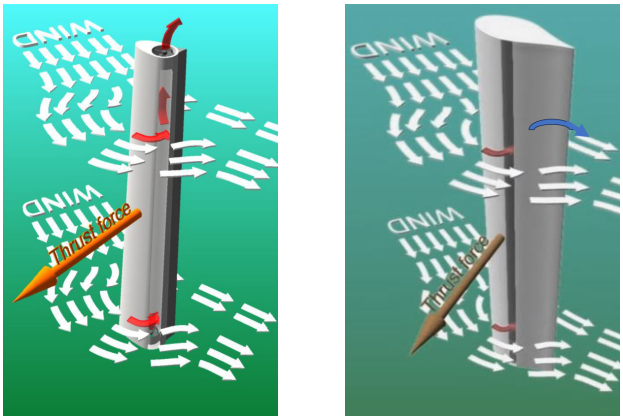

(a) VentiFoil **(b)** VentoFoil

Figure 2.2: Working principles comparison (Econowind, 2023)

The suction effect is illustrated in figure 2.3, where the upper figure is without suction and the lower figure is with suction. The van of the VentoFoil is positioned in the middle of the wing, pumping from the leeward to the luff side (blue arrow). This suction causes the streamlines on the leeward side to closely follow the surface, resulting in a higher lift force (red arrow). As a result, suction wings serve as a practical alternative to sails on cargo vessels, offering space-efficient wind propulsion.

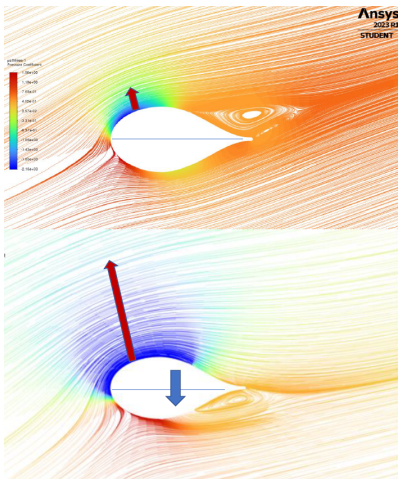

Figure 2.3: VentoFoil with (lower figure) and without (upper figure) suction at $AoA = 24^{\circ}$ (Econowind, 2023)

At the time of writing this report, the VentoFoils are being researched by Econowind and wind tunnel tests are being performed, however, these results have not been published yet.

2.2. VentoFoil Types

There are multiple sizes of VentoFoils shown in table 2.1. Depending on the size of the vessel and the available space on deck it is possible to choose a VentoFoil with a bigger span. The bigger the span, the higher the forces. The titling direction indicates whether it can be tilted down only on one spot (uni) or at every possible rotation (omni). The VentoFoils with a 50dm cord have not been built yet and it is not known which titling direction they will get. The base type corresponds to the foundation.

Table 2.1: VentoFoil Types

Chord [dm]	Span [m]	Tilting direction	Base type
28	10	Omni	-
			Baseframe
		Uni	Container
	13	Omni	-
			Baseframe
		Uni	Container
	16	Omni	-
			Baseframe
		Uni	Flatrack
			Container
50	18	-	Baseframe
		Uni	Tilting frame
	24	-	Baseframe
		Uni	Tilting frame
	30	-	Baseframe
		Uni	Tilting frame

2.3. Requirements for VentoFoil Adoption Model

The following requirements are described based on the demands formulated by Econowind. The requirements are sorted on importance. The main goal of the model is to be able to decide whether to install VentoFoils in a specific position or not. This decision will be based on financial and environmental results.

Requirement 1 - Technology Adoption Decision-support model
Based on the model, it should be possible for shipowners to decide on whether or not to install VentoFoils. This decision can be based on the financial or the environmental impact. For a specific placement options, the model will calculate the benefits resulting in one of the three following outcome possibilities:

- *Sail with VentoFoils at the same speed as the vessel did before.*
  In that case, the engine power can be reduced when the VentoFoils generate a forward resulting force. This will reduce fuel costs and emissions, however, the number of trips will stay the same. The cargo yield will slightly change due to the weight of the VentoFoils. In case of a new build, it might be possible to select a smaller engine. This choice should be made on the possibility that the vessel encounters enough wind to sail for a certain percentage of the time at the desired ship speed and occasionally at a slower ship speed.
- *Sail with VentoFoils at a higher speed, with the same engine power.*
  In this case, the fuel costs and emissions are not reduced, however, the vessel might be able to sail more trips per year. Despite a slight decrease in cargo capacity, there could be an increase in the yearly cargo yield.
- *Do not install VentoFoils.*
  This will be the default case, for which all the costs are estimated based on normal operation without using VentoFoils

For each possible outcome, it's important to clearly show the financial and environmental benefits, including changes in yearly profits and EEDI/EEXI, to help shipowners make an informed decision about installing the VentoFoils. The different placement configurations can be compared and the decision on their placement can also be made.

The force balance calculation is dependent on the placement of the VentoFoils on board. The spacing between the VentoFoils will influence the interaction. The model should be able to calculate the sum of the forces to be able to find a force balance based on the placement of multiple VentoFoils. Every placement option will be manually inserted by an engineer using the model, in a parameterized way. The model should not decide which placement option is the best, however, it will give a set of results for every placement option. For every ship owner, the choice will depend on the combination of results that matter to them.

The goal of the model should not be to optimize the placement. In most cases, the VentoFoil placement will be on an existing vessel. Since placing the foils on every spot on the deck is impossible, an engineer should select the placement option based on the vessel's general arrangement. All possible placement options will be analyzed within the model to find the most optimal placement option within the vessel's options.

Requirement 2 - Short computational time
Since the model is a technology adoption decision-support model, that stimulates ship owners to decide to install VentoFoils, it should be based on (limited) main vessel parameters. If ship owners are orienting on the possible WASP systems, they are likely to provide some main vessel parameters. However, they are probably not particularly enthusiastic about sending a lot of information about their vessel. For this reason, the model should be able to work with minimal input parameters and in a short computational time, which is likely low-fidelity.

The results from existing high-fidelity models should be implemented as simple force approximations, for example, to estimate the interaction between VentoFoils. The results from high-fidelity models can be implemented for all different configurations of VentoFoils, however, within the model, this should be with low computational time which has the tradeoff of low accuracy. Different sizes of VentoFoils will require the selection of known parameters for weight, span, chord, lift- and drag coefficients. The variation in footprint and van curve should be adjustable.

Additionally, the forces acting on the vessel equipped with VentoFoils should be calculated for different velocities. These forces occur under certain weather conditions, which will be an uncertainty, leading to a lower required fidelity level. Cost estimations do not require high fidelity due to the fluctuations in prices and margins.

Requirement 3 - Adaptable weather matrix
For the accuracy of the calculations, the weather data is important. For a vessel operating its whole lifetime in the same area, the world weather probability matrix of IMO (IMO, 2021) will not give relevant results. For that reason, it is a requirement that the model can adapt the results on the navigational area of the vessel. Since this is not the most important requirement, the focus will not be on the routing. For the EEXI/EEDI calculation, the worldwide weather data of IMO will always be used.

2.4. Conclusion

This chapter gave an overview of the working principle of VentoFoils, based on research conducted by previous graduation students. The requirements for a VentoFoil adoption decision-support model are defined. By doing so, it answered the following sub-question: *SQ1: What is the current status of VentoFoils research and development, and what requirements must be met for a model assessing their adoption and impact on the vessel's finances and emissions?*.

Research on VentiFoils was performed by Kisjes (2017), Lagendijk (2018) and Borren (2022). These are mostly high-fidelity models on the performance of the VentiFoil. Econowind has some CFD and wind tunnel test results on the performance of VentoFoils, however, these results are not published in papers. A large development step was made from the VentiFoil to the VentoFoil, however, the VentoFoils are only placed on a few vessels and the operational results are not known yet.

The three requirements are structured to enable the adoption and placement decision, considering both financial and environmental benefits. It should be a low-fidelity model because the available information is limited and the model aims to give an estimation of the different placement options. The model should have an adaptable weather matrix for more detailed calculations.

3

Existing wind-assisted propulsion models

This chapter dives into the existing wind-assisted models by answering the second sub-question: *"What existing models of wind-assisted propulsion are available, and what are the underlying mechanisms of each?"* To answer this question, thirteen models in the literature are described in detail in section 3.1, this includes the existing model at Econowind. In section 3.2 the models are compared based on the WASP systems utilized, the fidelity level they have, and the methods they use. Section 2.3 evaluates which requirements are met per model. In the conclusion, the research gap is described (section 3.3).

3.1. Detailed Analysis of Existing models

During literature research, a set of useful models was selected to assist in developing the model described in section 2.3. The criteria on which the models were selected were the following:

- The model should involve a WAPS. If it involves VentiFoils/VentoFoils specifically, it will be described.
- Models that calculate the forces and moments on a vessel equipped with a WAPS are selected. Especially models with low fidelity with the ability to calculate the forces and moments with minimal parameters. Financial models, evaluating the financial benefits of a WASP system are included.
- Decision-making models (on routing) are selected to learn about the decision-making process within the WASP industry. Models are only selected if they are relevant to the decision-making process of VentoFoils, models for Flettner rotors are similar, however rigid wing sails require other decisions.

Based on the above-presented criteria literature research was performed using Google Scholar. The theses from Lagendijk and Borren were found on the TU Delft repository. The Econowind model was received from Econowind. A researcher on WAPS at the TU Delft shared the links to the financial models. The following models are described in detail below:

1. Performance Prediction Program for Wind-Assisted Cargo Ships in section 3.1.1 (Reche-Vilanova et al., 2021)
2. ShipCLEAN model in section 3.1.2 (Tillig and Ringsberg, 2020)
3. xWASP_CN in section 3.1.3 (Charlou et al., 2023)
4. FPP in section 3.1.4 (Kisjes, 2017)
5. High-fidelity model VentiFoil in section 3.1.5 (Lagendijk, 2018)
6. High-fidelity model multiple VentiFoils in section 3.1.6 (Borren, 2022)
7. Decision-making process model in section 3.1.7 (Chica et al., 2023)

8. Routing model in section 3.1.8 (Bentin et al., 2016)
9. Real-time decision support model in section 3.1.9 (Müller et al., 2019)
10. Pelican Performance Prediction Software in section 3.1.10 (Van der Kolk and Bordogna, 2024)
11. Econowind model in section 3.1.11 (Lagendijk, 2018)
12. HHX.Blue model in section 3.1.12 (HHX.Blue, 2024)
13. WASP Decision Support Tool in section 3.1.13 (Kühne Logistics University, 2024)

3.1.1. Performance Prediction Program for Wind-Assisted Cargo Ships

Martina Reche-Vilanova (2021) developed the Performance Prediction Program (PPP) for Wind-Assisted Cargo Ships intending to create a more generic model than the existing ones, making it available for different WAPS with limited input parameters. The model integrates the aerodynamic and hydrodynamic forces acting on a vessel equipped with the three different types of WAPS: Flettner rotors, rigid wing sails (different flap configurations), and DynaRigs (figure 3.1). The model balances all forces and moments, with an FS-equilibrium workbench from the Fluid Engineering Department of DNV[1], containing two models: a hull model and one of the three WASP models.

The hull model accounts for gravity forces, buoyancy, and hydrostatics, along with hull resistance (calculated using the Holtrop and Mennen Method), side force in response to WASP aerodynamic loads, rudder hydrodynamic force, aerodynamic resistance of the superstructure, propeller thrust, and added resistance in waves. These forces act on the Centre of Effort (CoE) and are determined based on simple input parameters such as vessel main particulars. The CoE is calculated with basic geometry rules. The effect of the Apparent Wind Speed (AWS), Apparent Wind Angle (AWA), leeway angle, and pitch angle are also considered.

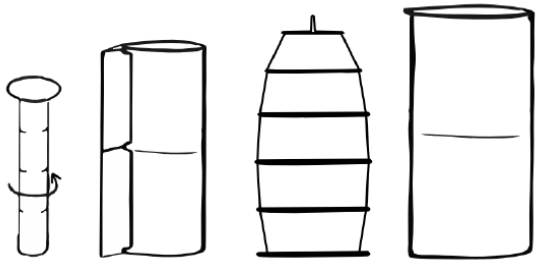

Figure 3.1: Comparison of different WAPS: proportional representation (Reche-Vilanova et al., 2021)

The WASP model employs simple estimations and data fitting, taking into account various aspects. It considers the true wind velocity profile. For Flettner rotors, the model involves extrapolating Jakob Ackeret results from (Prandtl and Betz, 1932) data, integrating aspect ratio (AR), endplate size factor (De/D), and velocity ratio (U/V) to determine representative lift and drag. Additionally, the model accounts for spinning power causing skin friction drag (R_F) and air resistance when the rotor sail is not rotating. Concerning Rigid Wing Sails, the WASP model considers aerodynamic lift and drag based on the linearised 2D form of Bernoulli's equation and the Kutta-Joukowski theorem. Different configurations are explored, incorporating flap deflection (d_{TF}) and flap cord ratio (C_{TF}/C_{RW}). For DynaRig, the model addresses aerodynamic lift, drag, and air resistance when they do not contribute to the thrust.

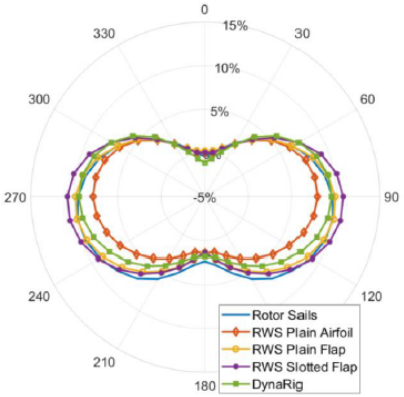

Figure 3.2: Absolute power savings of different WAPS for $V_s = 12.5\,kn$ and $TWS = 10\,m/s$ (Reche-Vilanova et al., 2021)

The model is validated using the data from the MAERSK PELICAN sailing with two NorsePower rotors. The other WAPS included in the model are not validated.

[1]This source was referenced in the thesis at DNV by Reche-Vilanova et al., but it is not a publicly available source.

A comparison among the three different WAPS (Flettner rotor, Rigid Wing Sail, and DynaRig) is made in the model across various wind speeds and sailing velocities. To ensure a fair comparison, efficiency is calculated per projected sail area. In figure 3.2 the absolute power saving of the different WAPS is shown. The rotors demonstrate the best performance in downwind and broad-reach courses, while the DynaRig shows greater potential in upwind sailing courses.

3.1.2. ShipCLEAN model

The ShipCLEAN model developers (Tillig and Ringsberg, 2020) aimed to provide an accurate performance prediction with very limited input data with short computational time. The model is a very complete ship performance prediction model based on analytical and empirical methods as well as on propeller and hull standard series. ShipCLEAN is a low-fidelity model in which computational efficiency is prioritized by employing only essential vessel parameters and avoiding complex time-consuming calculations such as CFD. Consisting of static and dynamic components the model is modular in design, allowing for the interchangeable integration of separate modules, as illustrated in figure 3.3.

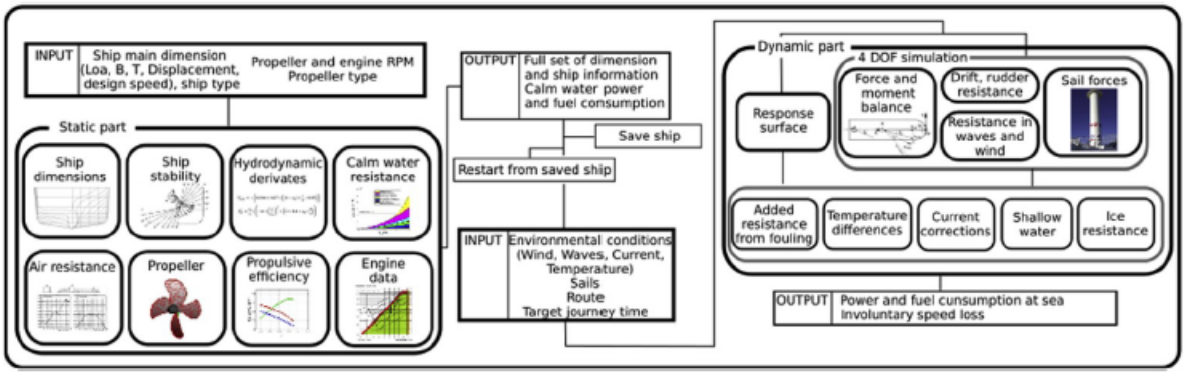

Figure 3.3: ShipCLEAN model overview (Tillig and Ringsberg, 2020)

Within the dynamic component of the model, alongside the static elements, a steady-state model is integrated, incorporating four degrees of freedom (DOF): surge, drift, heel, and yaw (Tillig and Ringsberg, 2019). This model ensures that the sum of all forces and moments is balanced. Due to the interdependence of the forces and moments, the solution is found through an iterative process. The minimum required propeller power is determined by iteratively adjusting the rpm control of the various Flettner rotors.

Inside the 4DOF simulation, the sail model represents the aerodynamics of the Flettner rotor. A wind speed gradient is used to describe the horizontal distribution of wind speed, with variations in both the angle and magnitude of wind speed occurring over height. The optimal rpm for maximum net power (thrust power minus consumed power) is found by evaluating the forces, power consumption, and moments of the rotors at several heights. The sail-sail interaction is not computed with CFD to reduce computational time; instead, a reduction in wind speed due to interaction is set to 5%. Meanwhile, the sail-superstructure interaction is simplified, modeling only the downstream wake with a sinusoidal reduction in wind speed (Peterka et al., 1985). This interaction was validated using values from the literature and the results show a good agreement although the model tends to be somewhat conservative at times.

The interaction between the sail and hull is crucial in understanding the dynamics of sailing. Estimating the lift coefficient (C_L) of the hull poses challenges due to the influence of the cross-flow drag coefficient (k'). However, the same value is used for lift as for drag calculations. Therefore the lift-to-drag ratio is less affected by k'. Consequently, the resulting drift angle from the lift-to-drag ratio does give a reasonably accurate prediction. Moreover, the hydrodynamic drag forces of the hull can be calculated with this ratio. Predictions regarding the CoE of the hydrodynamic drag forces are based on equations proposed in (Inoue et al., 1981). Additionally, enhancing the hydrodynamic side force of the hull is achievable by adding a center- or daggerboard. These boards require a high aspect ratio, enabling the calculation of lift and drag coefficients using equations from (Houghton et al., 2017) and (Hooft, 1994).

The ShipCLEAN model was validated with model tests and full-scale measurements, demonstrating a high level of agreement. A comprehensive case study was conducted involving a tanker and a Roll-on-Roll-off vessel, equipped with a total of 11 different arrangements of Flettner Rotors. Through this case study, fuel savings and payback time were assessed using realistic weather data. The findings underscored the significance of employing a 4DOF ship performance model, aero- and hydrodynamic interactions and individually controlling the rpm of each rotor to optimize performance.

3.1.3. xWASP_CN

Charlou et al. (2023) designed a open source numerical model, called xWASP_CN. The authors' goal was to make Dynamic Velocity Prediction Programs available as open-source tools. The model evaluates the performance of WAPS. It proposes a modular method with static and dynamic results in 6 degrees-of-freedom, that can be adapted to different design stages. The calculations can be performed for two different control strategies: Fixed speed (PPP) and Fixed propulsion (VPP). In the fixed speed strategy either the propulsion power or the engine speed is calculated. In the fixed propulsion strategy, the WAPS contributes to a higher vessel velocity.

The root finding algorithm (figure 3.4) is used to find the balance in forces ($\sum F = 0$ and $\sum M = 0$). The six degrees of freedom are divided into two separate problems: the horizontal problem ($\dot{x}$, $\dot{y}$ and ϕ) and the hydrostatic problem (z, ϕ and θ), due to negligible coupling between them. However, significant coupling exists within each problem. The global problem includes all forces acting on the ship, both horizontal and vertical, and is solved as a coupled problem.

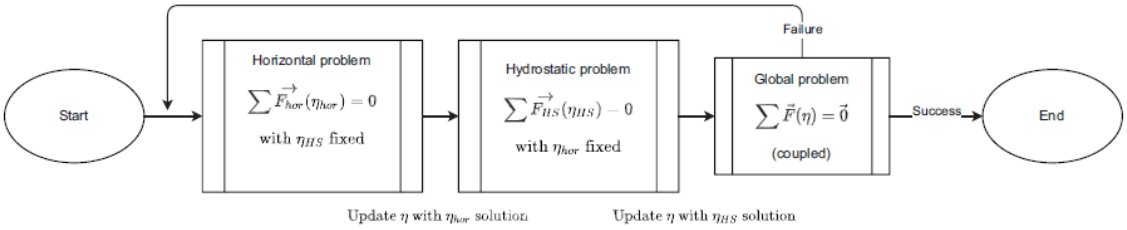

Figure 3.4: Root finding algorithm (Charlou et al., 2023)

The model was validated with an 18ft catamaran equipped with a Flettner rotor and a water turbine. For beam reach conditions, the longitudinal forces were in the right order of magnitude, but the side forces seem hard to predict with this model.

3.1.4. Fuel prediction program (FPP)

Kisjes adjusted a fuel prediction program (FPP) with CFD results of a turbosail as his graduation project (2017). The goal was to find the effect of a turbo sail on the fuel consumption of an existing vessel. The FPP consists of 3 motion equations: $\sum F_x = 0$, $\sum F_y = 0$, and $\sum M_z = 0$, in which he included the wind forces on the superstructure, the rudder forces, the resistance, the thrust force and the force of the turbo sails. A matching procedure was performed for a specific B-series propellor. The fuel consumption was calculated with the specific fuel consumption, varying for different engine speeds.

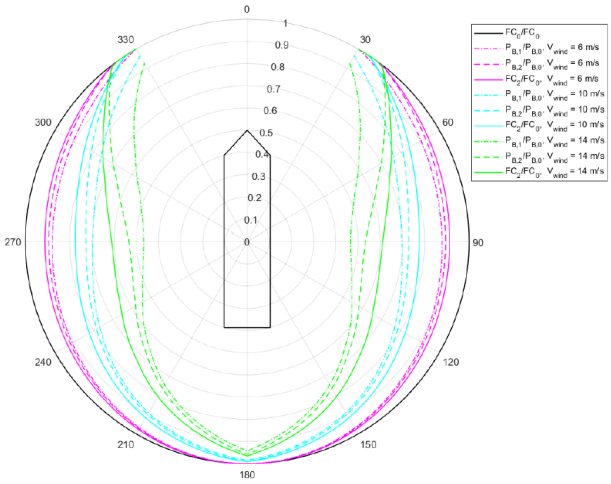

Figure 3.5: The reduction in brake power of the propellor and/or fan and the total fuel consumption using WASP as a ratio of the original case without WASP (Kisjes, 2017).

After performing a CFD analysis on the 2D (SRANS and URANS) and 3D (SRANS SST and SRANS EARSM) effects of turbo sails,

the lift- and drag coefficients are implemented in the calculations for the FPP. The aspiration power of multiple vans was calculated and compared. As a result, the reduction in brake power and fuel consumption could be shown in a diagram shown in figure 3.5. The power of the turbo sail was determined with $P = F \cdot V_s$, which as explained in section 4.3.6, is not valid for wind-assisted vessels.

Since this thesis was performed at the beginning of Econowind, the data and design of the VentiFoil were not validated and optimized yet. Therefore, the results are outdated, however, the method can be partly used for building the adoption decision-support model.

3.1.5. High-fidelity model VentiFoil

Laurens-Jan Lagendijk (2018) built several CFD models for the VentiFoil at Econowind in which he researched the following components: the hole diameter and distribution, the 2D shape of the VentiFoil, the 3D effects on the VentiFoil, the effect on the height of the VentiFoil, the possible endplate position, the interaction of two VentiFoils. The goal of these models was to find the ultimate VentiFoil design based on the mentioned parameters

In the paper, it is concluded after CFD modelling that round holes with small diameters perform best. The benefits of round holes include less resistance with respect to other shapes, easier production, and a reduction in the diameter of the holes resulting in improved pressure distribution. Turbulence in this CFD model is represented by the Reynolds Averaged Navier-Stokes (RANS) mathematical model, using Shear Stress Transport (SST) to model turbulence. Numerical discretization is employed to solve the Navier-Stokes equations. For this model, an uncertainty assessment was performed to determine the reliability of the solutions.

A 2D CFD model was employed to determine the optimal shape of the VentiFoil. Generally, a larger flap angle generates more thrust, although its effect is minor. Increasing the flap length increases the effective area, thus improving performance. Variation in the leading edge parameter shows that a pointed leading edge, characterized by a reduced edge curvature, is less prone to stall, resulting in enhanced performance. A higher thickness ratio provides a larger surface area upon which pressure acts. Consequently, smaller leading edge curvatures require less suction to maintain flow attachment, leading to improved performance. A larger surface area offers the highest efficiency, indicating that a taper is not preferable. A VentiFoil without taper, fitting tightly in a container, provides more area. Parameter variation indicates that suction locations closer to the trailing edge significantly enhance performance, particularly for large suction coefficients.

In a 3D model, Lagendijk investigated the influence of tip effects on span variation and end plate position. The tip effects are most significant for VentiFoils with small spans. The end plate should be positioned in a way that it covers the top of the leeward side, where the low pressure is located. This can be done by a rotating end plate or an end plate that covers the top of the VentiFoil on both sides.

Lastly, a 3D CFD model was used to evaluate the influence of the interaction between two VentiFoils. They are located next to each other causing the most wake disturbance in beam reach condition. For conditions where there is interaction, the second VentiFoil should be placed under another angle of attack than the first VentiFoil.

After all the CFD research performed on the VentiFoil Lagendijk proposes a new design of the VentiFoil that results in an improved thrust of 5.2%.

3.1.6. High-fidelity model multiple VentiFoils

Mark Borren (2022) developed a Computational Fluid Dynamics (CFD) model to analyze the interaction between multiple VentiFoils. Using the Lifting Line (LL) theory of Prandtl, he estimated the 3D forces, based on 2D RANS simulations for the discretized parts. The LL model was validated with a 3D RANS CFD model. These 3D RANS simulations provided valuable insight into the complex aerodynamic interactions between VentiFoils, complementing the simpler yet faster LL model calculations.

In Borren's model, two VentiFoils were positioned next to each other on an invisible deck at varying relative distances ($D_R = 3.5 \cdot c$ and $D_R = 7 \cdot c$). Analysis of the simulations revealed influence between the VentiFoils under all apparent wind angles, with the greatest effect observed at a 90-degree angle, where the VentiFoils are parallel to the flow. As the relative distance increased, the interaction between

the VentiFoils decreased.

Optimization of the thrust coefficient C_X is achievable by adjusting the angle of attack of the downstream foil. With a relative distance of $D_R = 7 \cdot c$, marginal absolute differences were observed, as can be seen in figure 3.6. However, a significant difference persisted at the apparent wind angle $\beta_a = 90°$. Furthermore, both VentiFoils together outperformed the single VentiFoil at high angles.

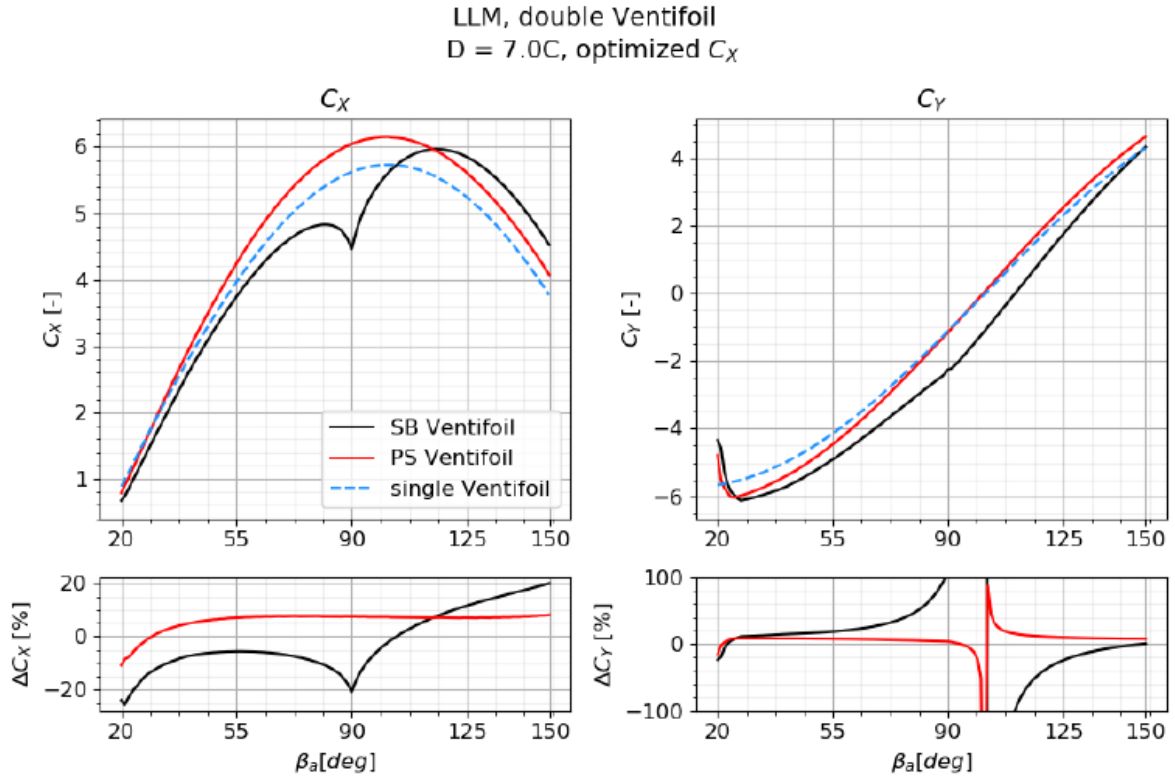

Figure 3.6: Lift and drag coefficient over apparent wind angle (Borren, 2022)

The optimized angles are shown in figure 3.7. To obtain this optimized C_X the downstream VentiFoil is set at a maximum effective angle of attack of $\alpha_e = 30°$, the angle from which stall occurs. The effective angle α_e becomes smaller near $\beta_a = 90°$.

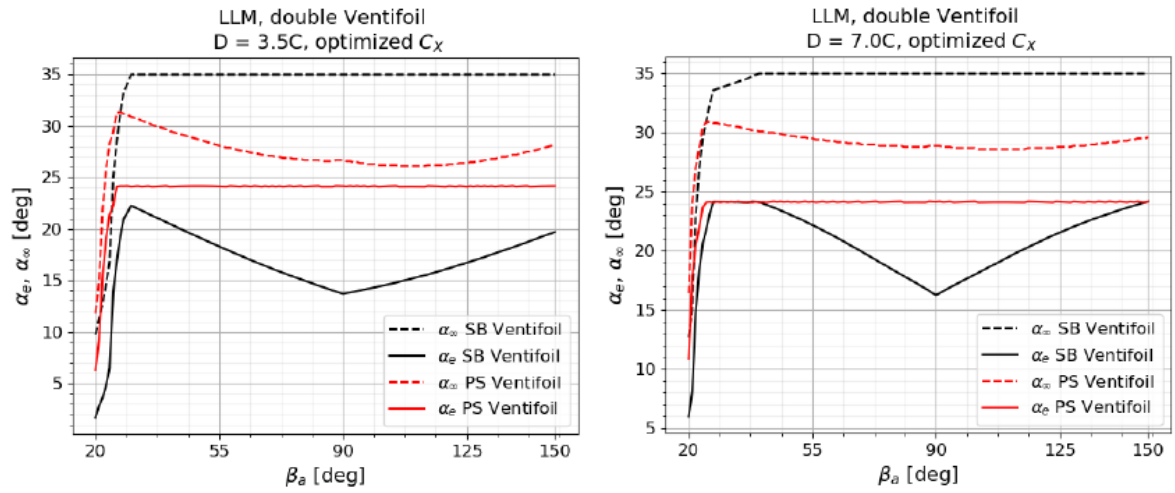

Figure 3.7: Adaptive operational guideline of the angle of attack of the downstream VentiFoil (Borren, 2022)

3.1.7. Decision making process model

In the agent-based decision-making (ABM) process model by Chica et al. (2023), three WAPSs are considered: Flettner rotors, Wingsail twinfoils, and VentiFoils. The model aims to find the most effective policy or intervention leading to a higher adoption grade of WAPSs. Within the ABM the awareness of the WAPSs is modeled and the possible utility over time that an agent perceives from a WAPS. In this model, the awareness of the agent is taken into account as well as the lifetime of the vessel, the environmental benefits, the costs, and the savings of the WAPS. These steps are illustrated in the diagram shown in figure 3.8 The awareness is modeled with the Bass model. Per time step the utility of the WAPS is calculated and when their utility is > 0 the WAPS with the highest utility is adopted.

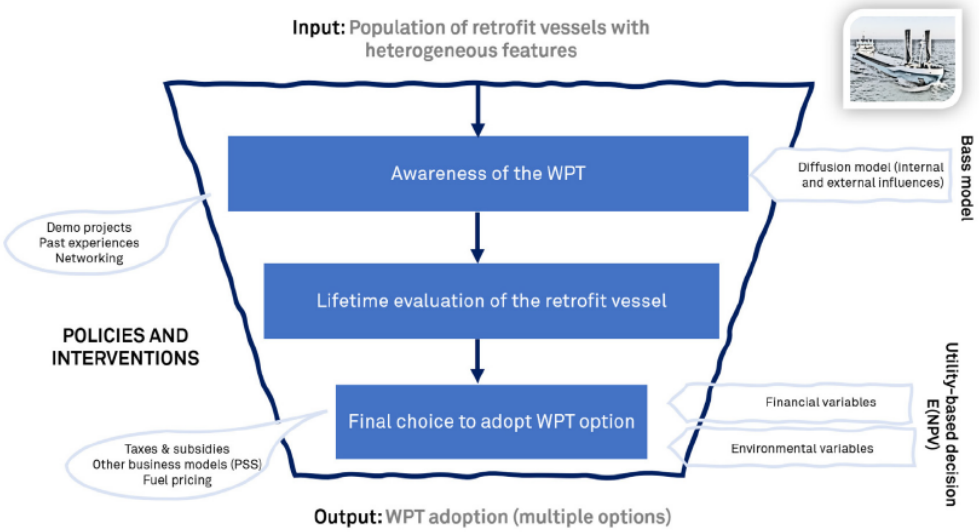

Figure 3.8: Agent-based model (ABM) for Wind Propulsion Technology (WPT) adoption (Chica et al., 2023)

For 6009 ships the simulation of 30 years was run for two scenarios: a monthly increase in fuel price of 0.5% and a yearly increase in fuel price of 5%. The adaption of fuel taxes and a subsidy of €275.000 for installation costs results in the graph shown in figure 3.9. The VentiFoil is adopted approximately 30 times more than the Wingsail and approximately 100 times more than the Flettner rotor. The VentiFoil has, according to this research, also the lowest installation costs, but the lowest fuel reduction rates. For Wingsails a higher subsidy would increase the adoption to 5%, when considering 10% of initial awareness, 43, 000 nm sailing distance, installation cost subsidies, and yearly fuel price updating. The combination of networking effects and installation subsidies can lead to significant adoption of a WAPS and give guidance in promoting its adoption.

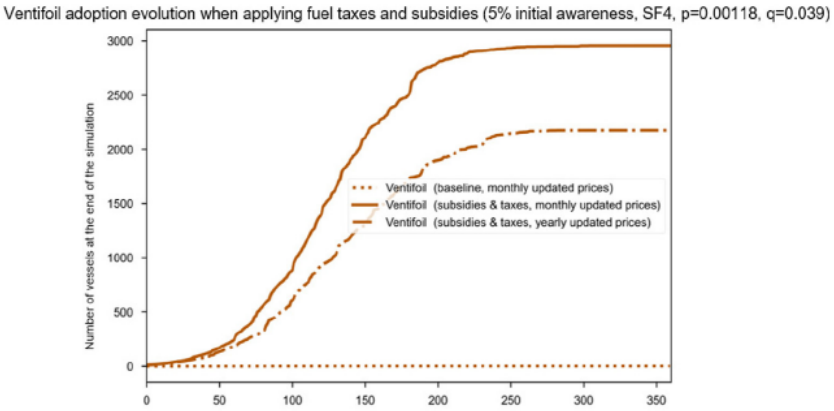

Figure 3.9: Ventifoil adoption evolution (Chica et al., 2023)

3.1.8. Routing model

In a study by Bentin et al. (2016), a routing tool was developed for the BBC Hudson, a bulker/multipurpose carrier. This tool aimed to minimize energy consumption, considering wind, waves, and the contributions of a WAPS. The A^* search algorithm was used to generate a tree of potential routes, considering varying wind and wave conditions for each route. The optimization was applied to the route from Baltimore (USA) to Wilhelmshaven (Germany), simulated daily for over a year. Results indicated that route optimization could reduce energy consumption by 53%, with the WAPS alone offering a 36% reduction. Routing optimization contributed approximately 5-8% to this effect. However, this optimization led to a 6-10 hour increase in travel time, which stays within the research margin.

The paper also discusses the inclusion of other WAPSs (Kite, Flettner, and DynaRig), but only the Flettner results were evaluated. Economic efficiency calculations are challenging due to the system's strong dependency on the WAPS and market developments.

3.1.9. Real-time decision support model

Müller et al. (2019) developed an intelligent assistance system for real-life decision-making and automated rotor speed on a vessel equipped with Flettner Rotors. The aim is to automate the Flettner rotor operation and to be able to store the data to optimize the system. A graphical user interface (GUI) was used to provide the crew onboard with the tools to get insight into power reduction possibilities. For the current windspeed and true wind angle, the dynamic polar chart is drawn (figure 3.10). The crew can see the real-life saving potential by changing the course. The model makes use of sensors and saves all the measured data to improve the system's calculations.

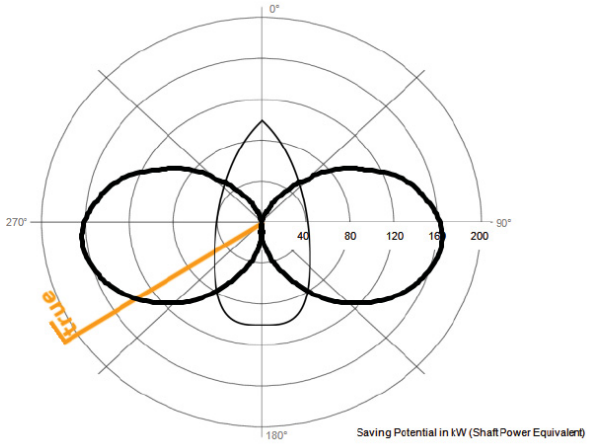

Figure 3.10: Dynamic Polar Chart (Müller et al., 2019)

The paper focuses mainly on the interface, control systems, and data storage possibilities. The calculations regarding the Flettner rotors are quite limited within the paper.

3.1.10. Blue WASP: Pelican Performance Prediction Software

Van der Kolk and Bordogna, from Blue WASP (2024), developed a model called Pelican Performance Prediction Software, that aims to compare different WAPSs fairly. Because it is a commercial model, the detailed method and calculations are not published. With the Pelican Performance Prediction Software, it is possible to calculate the performance of a vessel equipped with Flettner rotors, Wingsails, Turbosails, or Kitesails at a specific route. Together with the developers of the model, it is possible to optimize the fuel savings, route, and speed of the vessel.

The model consists of multiple built-in force modules that are combined in an optimizer that has the goal of maximizing the net sail power. The aerodynamics force module is based on data from Flettner rotors, Wingsails, Turbosails, and Kitesails. The hydrodynamics model is trained with artificial intelligence (AI) to interpolate data from 1500 CFD simulations of different hull types. The model is built with high flexibility to adjust to specific vessels or systems.

3.1.11. Existing model at Econowind

At Econowind a model is used to estimate the power delivered by the VentoFoils. For every true wind speed (U_t) and true wind angle (β_t), the apparent wind speed (U_a) and angle (β_a) are calculated depending on the vessel's velocity (V_s). With that information matrix, the force in the X and Y directions can be calculated from the lift (L) and drag (D) equations given in equation 3.1 and 3.2 respectively.

$$L = \frac{1}{2} \cdot \rho_{air} \cdot C_L \cdot U_a^2 \tag{3.1}$$

$$D = \frac{1}{2} \cdot \rho_{air} \cdot C_D \cdot U_a^2 \tag{3.2}$$

The propulsion power is calculated with equation 3.3. It is derived from the general equation $P = F \cdot V$, where V is the ship speed V_s, however, this equation is only valid if the force of the VentoFoils is the only force (Hermans, 2024). In the model proposal, another method is suggested to find the propulsive power of the VentoFoils (equation 3.3). The second part of the equation is the fan power shown in figure 3.11. The fan power is turned off when the VentoFoil is not used, at very high and low apparent wind speeds. From U_{rated} till U_{max} the fan power is maximal (P_{rated}). Between U_{min} and U_{rated}, the fan power is calculated with equation 3.4. The propulsion power is shown in a polar plot (figure 3.12).

$$P_p = \frac{F_X \cdot V_s}{\eta_D} - P_{fan} \tag{3.3}$$

$$P_{fan} = \left(\frac{U_a}{U_{rated}} \right)^3 \cdot P_{rated} \tag{3.4}$$

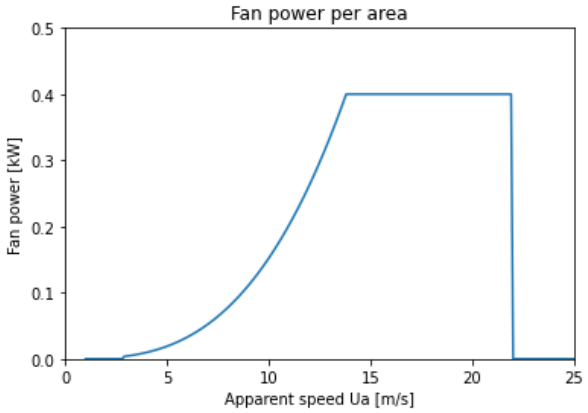

Figure 3.11: Fan power

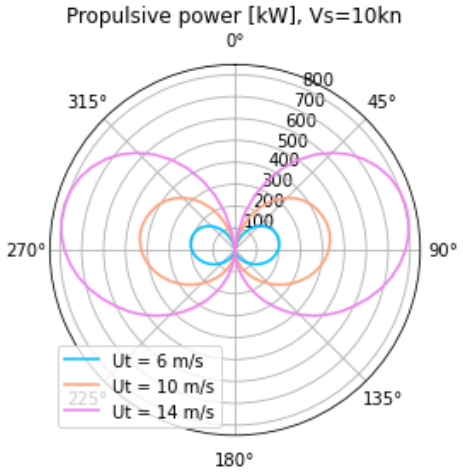

Figure 3.12: Propulsive power of a VentoFoil

With the polar plots for fan power and driving force, the EEXI can be calculated. The wind probability matrix of the IMO is used to calculate the EEXI with equation 3.5 as the guideline. This part of the equation represents the wind-assist part of the bigger EEXI equation. $W_{i,j}$ is the wind probability for different wind speeds and angles. The same steps as in the polar model are used to calculate the apparent wind speed, apparent wind angle, force, and fan power. The reference speed is the ship speed, which remains constant within this model. η_D is the total efficiency of the main driver(s) at 75% of the rated installed power (MCR) of the main engine(s) and is set to 0.7 if no other value is specified (IMO, 2021).

$$(f_{eff} \cdot P_{eff}) = \left(\frac{1}{\sum_{k=1}^{q} W_k} \right) \left(\left(\frac{0.5144 \cdot V_{ref}}{\eta_D} \sum_{k=1}^{q} F(V_{ref})_k \cdot W_k \right) - \left(\sum_{k=1}^{q} P(V_{ref})_k \cdot W_k \right) \right) \tag{3.5}$$

The calculations performed in this model can be done for different sizes of VentoFoils but are not yet adapted to multiple foils, placed at a certain distance and angle from each other. The polar plot only exhibits the effect of the VentoFoil, not the interaction with the vessel and the placement on the vessel. The effect of Angle of Attack (AoA) is not considered. In the calculations for the propulsive power, the fact that the VentoFoils will be folded down if $P_p < 0$ and if the windspeed is too high is taken into account.

3.1.12. HHX.Blue model

The HHX.Blue model consists of a technical selection and financial model (HHX.Blue, 2024). The technical selection model will scale the options to not take action, to install a WAPS system or to install a non-WAPS technology based on the Analytic Hierarchy Process (AHP). This method bases its scaling on criteria for which the user has to fill in the level of agreement. To grade the agreement of a criterium, background information on the financials, technical solutions and commerciallity should be available. The model does not include this background, however, the company explains: "...the feeling and assessment of the expert using this tool is sufficient at this stage."(HHX.Blue, 2024).

The financial model (HHX.Blue, 2024) calculates the Net Present Value (NPV) of the WAPS system for the owner and the technical provider. Comparing these two will result in the fairness of the deal. If the NPV for both parties is positive, the deal will be fair, otherwise, the deal is unfair. If the deal is not fair, the input can be changed by negotiating about the advance payment, carbon price, fuel price and savings. The model includes matrices for these four pillars, giving the influence of changes. For this model, the input consists of the key points of the agreement and the key technical data.

3.1.13. WASP Decision Support Tool

The WASP Decision Support Tool (Kühne Logistics University, 2024) calculates the financials of the following technologies: flettner rotor, suction wing, rigid sail and kite. Although the author of the tool is not known, the model was created as a collaboration between Kühne Logistics University, CSGL and Interreg, a European Development fund for WASP. The input parameters can be inserted based on vessel dimensions, lifetime and operational profile. The expected wind and sea current effects can be adjusted based on the route. The financial and operational data of the technologies can be changed depending on the type of technology, including factors such as its size and the manufacturer. There are already values in the model, for all four technologies and vessel types, however, it is unknown if these are from existing or average technologies and vessels.

The outcomes are the financial comparisons between the four technologies. One of those outcomes is the NPV, which is calculated with two different methods. Because the tool does not provide any information about how its calculations are done, it is impossible to understand, verify, or compare its method with other methods, including the one built in this thesis. Without knowing how the tool works, it cannot be reliably used or analyzed, so it was excluded from this study.

3.2. Comparison and Evaluation

To enable comparison among these models, table 3.1 indicates the WAPSs for which the model is built, its fidelity level, and what method is used for the calculations. The requirements for the model for this research as listed in section 2.3 are placed in the last column of the table. The symbols (✓) and (**X**) indicate whether the requirements are met or not, respectively. (✓/**X**) means that a requirement is only partly met.

Table 3.1: Comparison of the existing models

Model	**Type of Wind-Assisted Propulsion System**	**Fidelity level**	**Method**	**Meets requirements**		
				RQ1	RQ2	RQ3
PPP	Flettner rotors Rigid Wing Sails DynaRigs	Low	Data-driven Semi-empirical	**X**	✓	**X**
ShipCLEAN	Flettner rotors	Low	Analytical- and empirical methods Hull standard series	**X**	✓	✓
xWASP_CN	Modular model for multiple WAPS	Low	System based modelling Root-finding algorithm	**X**	✓	**X**
FPP (Kisjes)	Turbosails	High	Computational Fluid Dynamics	✓/**X**	**X**	**X**
Multiple VentiFoils (Borren)	VentiFoil	High	Lifting Line Model	**X**	**X**	**X**
VentiFoil model (Lagendijk)	VentiFoil	High	Computational Fluid Dynamics	**X**	**X**	**X**
Decision making process model	Flettner rotors Wingsail twinfoil VentiFoil	Low	Agent-based simulation model	**X**	**X**	**X**
Routing model	Kitesails Flettner rotors DynaRig	Low	$A*$ search algorithm	**X**	✓	✓
Real-life decision-making support model	Flettner rotors	Low	Simple force calculations	**X**	✓	**X**
Pelican Performance Prediction Software	Flettner rotors Wing-, Turbo-, and Kitesails	Low	Data-driven Built-in force model	✓/**X**	✓	✓
Econowind model	Venti- and VentoFoils	Low	Simple force calculations Energy Efficiency Existing Ships Index	**X**	✓/**X**	✓
HHX.Blue Model	Every WASP system	Low	Analytic Hierarchy Process Financial calculations	**X**	✓	**X**
WASP Decision Support Model	Flettner rotors Suction wing Rigid Sail Kite	Low	Unknown	**X**	✓	**X**

The PPP (Reche-Vilanova et al., 2021) and the ShipCLEAN (Tillig and Ringsberg, 2020) models focus on minimal input parameters (RQ2) and can be adjusted for several placements of WAPS. The method used for estimating the forces and moments on the vessel can be used from these two models. The ShipCLEAN model has adjustable weather matrices (RQ3). They both do not focus on decision-support and do not include costs (RQ1).

The xWASP_CN (Charlou et al., 2023) model does calculate the forces on the vessel equipped with a WAPS (RQ2). The model does not use weather data, making it impossible to accurately estimate fuel savings where the probability of weather conditions is relevant (RQ3).

The fuel prediction program (FPP) (Kisjes, 2017) does not support the decision-support process, however, it does compare the case with and without turbo sails (RQ1). It is a low-fidelity model in which high-fidelity results are implemented, making it a high-fidelity model with specific propeller and rudder data (RQ2). No navigational data is used, probability is therefore not included in the model (RQ3).

Although the high-fidelity models do not meet any of the requirements, the results from those models can be used to estimate the forces on the VentoFoils. The results can be implemented in the low-fidelity

model. The interaction between the foils is investigated with the Multiple VentiFoils model of Borren (2022).

The decision-making process model (Chica et al., 2023) focuses on technology adoption at a higher level. It does not take into account the individual shipowner's decision, however, it looks at the general adoption after implementing different policies (RQ1). The other two requirements are not met.

The routing model (Bentin et al., 2016) makes decisions regarding routing, rather than handling the technology adoption decision stated in requirement 1 (RQ1). The route optimization process relies on force calculations of a vessel equipped with Flettner rotors (RQ2). The model is based on a specific route, it can be manually adjusted to other routes (RQ3).

The real-life decision-making support model (Müller et al., 2019) does not support the technology adoption decision (RQ1). It is a low-fidelity model based on basic vessel parameters (RQ2). The weather is not included in the model, however, the weather data is measured to validate the calculations (RQ3).

The Pelican Performance Prediction Software (Van der Kolk and Bordogna, 2024) makes a comparison between different WAPS to simplify the choice of the shipowner which technology they should adopt, however, it does not include the cost advantages of different systems and possible changes in operational profile (RQ1). It is a low-fidelity model with high flexibility (RQ2). The model focuses on specific routes (RQ3).

The existing Econowind model (Lagendijk, 2018)does not involve detailed decision-making (RQ1). The force calculations are made for the VentoFoils themselves, however, it does not consider the vessel and thus the moments (RQ2). The weather matrix is exchangeable (RQ3).

The two financial models (HHX.Blue, 2024 and Kühne Logistics University, 2024) do support the decision-making, however, it is not dependent on the placement on board and more focussed on the financial agreements (RQ1). They have a short computational time and require minimal input (RQ2). The specific wind condition can be inserted but does not involve probabilities (RQ3).

In summary, there are multiple models that partially meet the requirements (set in section 2.3). For this research, the available information on some of the models (the PPP model, the ShipCLEAN model, the high-fidelity models, and the Pelican Performance Prediction Software) can be used to extend the existing Econowind model to meet all the requirements. The model proposed within this research will be described in chapter 4.

3.3. Conclusion

A detailed description of the existing models related to the model that will be built within this research is given. Thereby the following subquestion is answered: *"What existing models of wind-assisted propulsion are available, and what are the underlying mechanisms of each?"*. The models are selected based on the criteria described in section 3.1. Per model, the underlying principles are described. A comparison between the models is made in table 3.1. The table also illustrates that none of the models meet all of the requirements. The models which meet most of the requirements are focussing on other WAPS, such as Flettner Rotors, and do not include the financials.

The existing literature on wind-assisted propulsion models has primarily focused on force balances, high-fidelity models, and operational decisions. However, a noticeable gap remains in technology adoption decision-support models based on financial benefits, which remains relatively unexplored. For ship owners, the financial and environmental impact of VentoFoil placement will be the main driver for their adoption decision. This research aims to fill this gap by building the VentoFoil adoption decision-support model described in chapter 4.

4

VentoFoil Adoption Model

The VentoFoil Adoption Model involves selecting a specific position for the VentoFoils on deck, which can be varied. The model then calculates the forces with and without the VentoFoils at that position, followed by a cost-benefit analysis. The forces are calculated for every possible combination of wind direction and speed, and then multiplied by their respective probabilities. This way a fair comparison between placement options can be made. The results are shown for three situations: normal operation without VentoFoils (baseline), VentoFoil operation at reference speed, and VentoFoil placement at reference power and thus higher speed. This tool is designed for use by naval architects in cooperation with the ship owner, enabling them to make well-considered decisions on whether and where to place the VentoFoils. This chapter described the calculations used in this model and the background information to answer subquestion 3: *'How can an early-stage VentoFoil adoption decision-support model be developed to model the force balance of VentoFoil placement on a vessel under varying weather conditions and assess their financial and environmental benefits?'*.

The model is graphically shown in figure 4.1 and will be described below per (calculation) step in the following sections. It is also described if parts of existing models are used within a calculation step.

The model consists of the input, baseline calculations, VentoFoil calculations, the comparison and the output. In the baseline calculation, the forces on the vessel are calculated without VentoFoils on board. This includes the resistance, thrust and wind forces on the deckhouse. The same calculations are performed for the VentoFoil calculations, however, the VentoFoil forces including interactions are added. The calculation is looped to find the case in which the power is the same as in the baseline calculations. The costs and benefits are calculated and compared for all three cases. The comparison will be shown visually in the output.

4.1. Wind probability matrix (Input)

The wind probability matrix provides input data that includes the probabilities of different wind directions and speeds for a given navigational area. The IMO made a global wind probability matrix, which is mandatory for EEXI calculations (IMO, 2021). However, for vessels operating in specific regions, the results differ if a regional matrix is applied. It is possible to replace the global matrix with one specific to the area. Due to the wide variety of possible routes and navigational regions, the specific matrices for all areas are not pre-loaded in the model. The matrices for different routes can be extracted from the Blue Route tool from MARIN (2024) which have the same format as the IMO matrix.

4.1.1. Windgradient

The wind gradient describes the increase in wind speed with altitude and can be calculated at a specific height using equation 4.1. In the IMO matrix and the matrices from Blue Route a Hellmann exponent of 0.14 is used at the reference height of 10 m (IMO, 2021 and MARIN, 2024). The graph resulting from

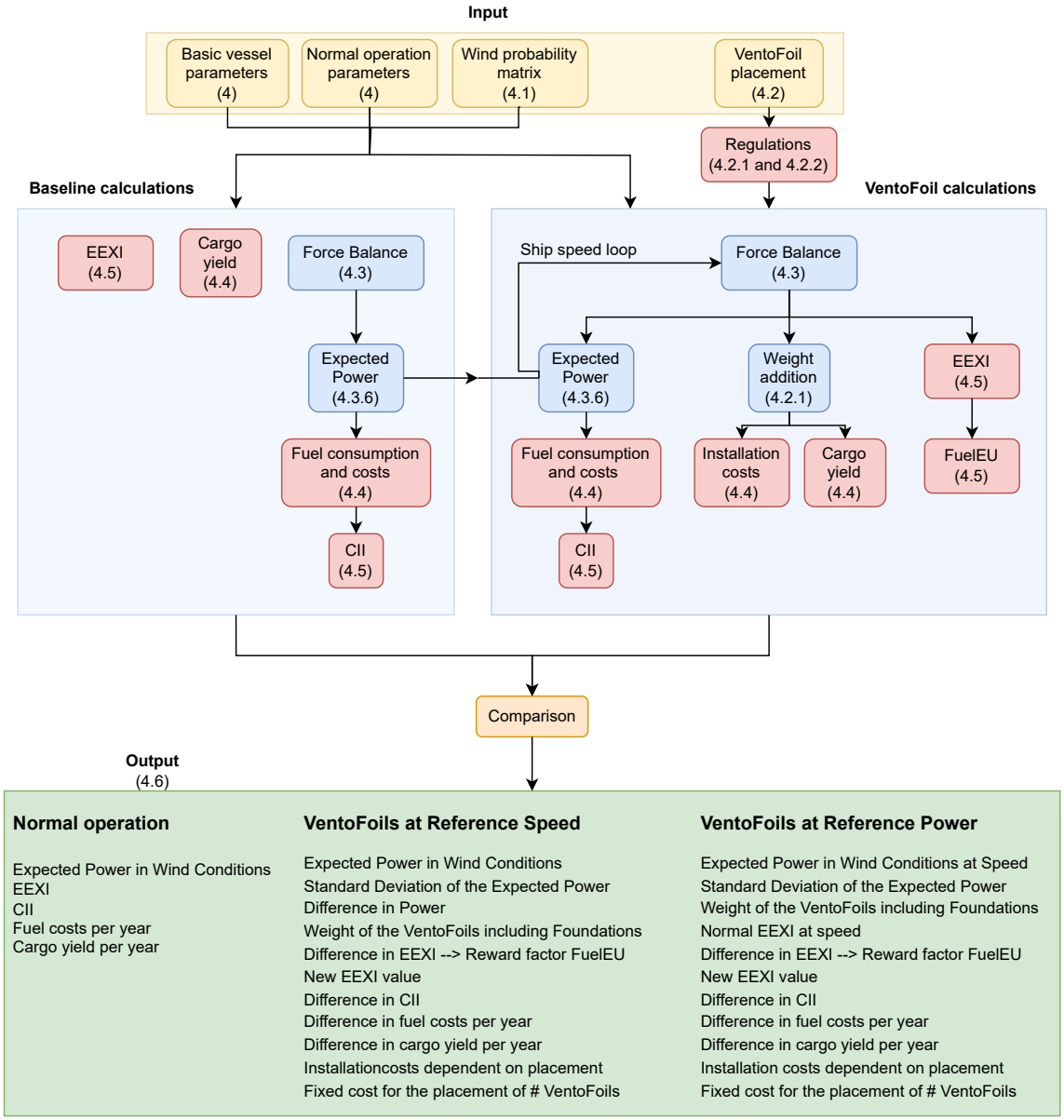

Figure 4.1: Flowchart of the VentoFoil Adoption Model

this equation is shown in figure 4.2.

$$v_{z_{ref}} = v_{10m}\left(\frac{z_{ref}}{10}\right)^{\alpha} \quad \text{for } z_{ref} < 300\,\text{m} \tag{4.1}$$

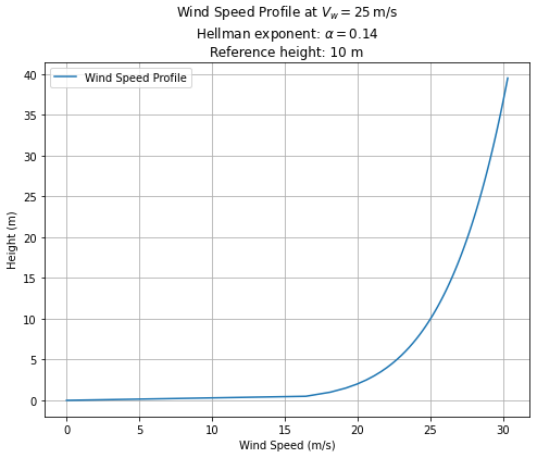

Figure 4.2: Wind speed profile

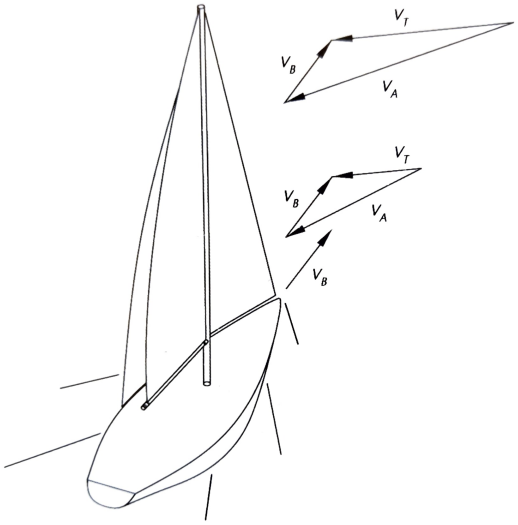

Figure 4.3: Apparent wind angle change over the height (Marchaj, 2003)

The ship does not have a fixed wind speed, however, the calculation loops over fixed sailing speeds. For a fixed sailing speed the wind gradient results in a varying apparent wind angle over the height as shown in figure 4.3. In the model, a discretization method is used: the span is divided into elements, and for each element, the wind speed and angle are taken at the Center of Effort (CoE). The height of the elements is set to 1,5 m but can be adjusted to improve the accuracy of the calculations.

4.2. VentoFoil Placement (Input)

The placement options for VentoFoils are parameterized. It is possible to place one or two VentoFoils per row. When one VentoFoil is placed in a row, it can have an offset value in y-direction. When two VentoFoils are placed in one row, they are placed symmetrically around the centerline. There is no maximum amount of VentoFoils that can be placed on the deck, however, the visibility regulations described in section 4.2.2 do limit the amount of VentoFoils, depending on the size of the vessel and the placement. In figure 4.4 an example is shown with its input values. Depending on the number of rows and the number of VentoFoils a certain amount of lengths, breadths and offset values are required. For each row, the height of the Ventofoils can also be adjusted. Before running the calculations in the model the placement can be checked by clicking the button ”Calculate Positions” and a visualization of the VentoFoil placement is shown in the three views: ‘Elevation view’, ‘Section view’ and ‘Plan view’ (figure 4.5).

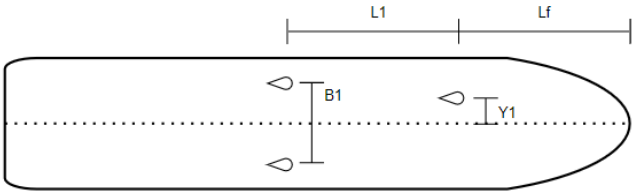

Figure 4.4: Placement example VentoFoils

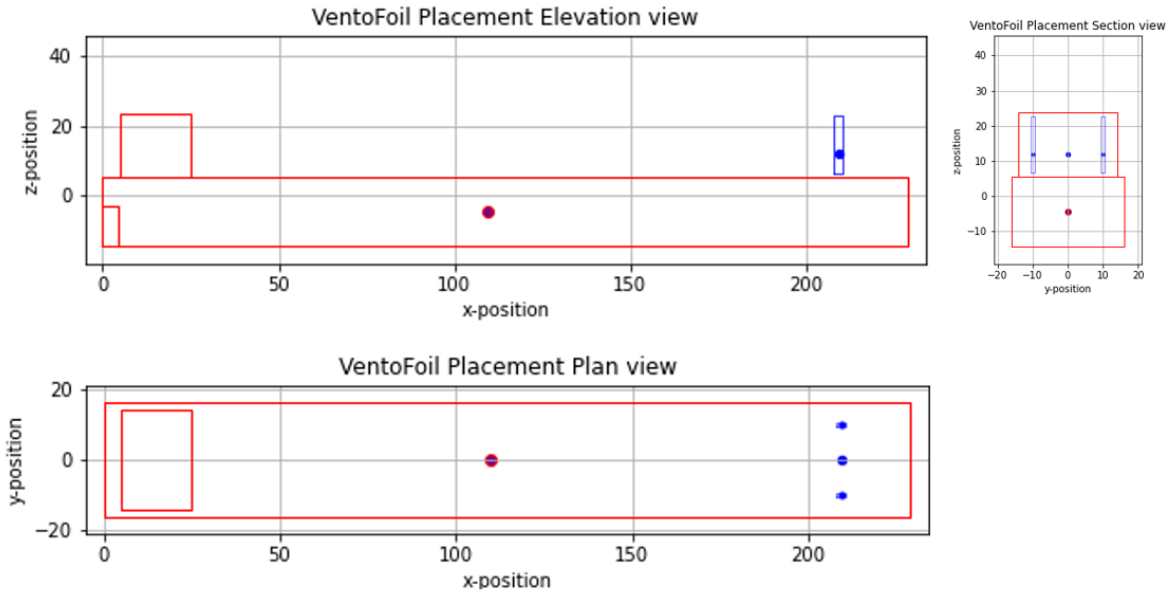

Figure 4.5: Example of the elevation, section and plan view of the VentoFoil placement in the model. The red dot is the centre of gravity (CoG) of the vessel without VentoFoils. The blue dot is the CoG of the VentoFoils and the purple dot is the CoG of the vessel including VentoFoils.

In addition to the choice of where to place the VentoFoils, the naval architect can select a VentoFoil type including tilting direction and base type. All combinations of chord, span, tilting direction, and base type are included in the model. However, only one type of foundation is implemented in the model to give an estimation of the weight and costs of foundations in general and to show that foundations can be implemented in the model. Some VentoFoil types are still in the design phase at Econowind, the details of coefficients and finances are therefore not available, as a result only the 16-meter and 30-meter VentoFoil are implemented in the model. In this first version of the model, only one type of VentoFoil can be placed onboard per calculation, as the interaction calculations only account for interactions between similar VentoFoils. Depending on the type of VentoFoil chosen, the forces, costs and weights can vary.

When a VentoFoil location is specified in the model, the first check is whether this location is allowed. This depends on the weight change or the centre of gravity change (Intact stability), and the obstructed visibility by the VentoFoils. These two factors are discussed in two subsections below.

4.2.1. Regulations: Intact stability

The IMO (2024) states that, in the event of significant modifications affecting a vessel's stability, such as changes in the vertical centre of gravity (VCG), longitudinal centre of gravity (LCG) or changes in lightweight of the vessel, the stability calculations must be recalculated and, if necessary, a new incline test must be performed. A warning message is added to the model if the changes in VCG, LCG, and lightweight exceed the threshold values shown in table 4.1.

The general formula used for a change in centre of gravity (CoG) is equation 4.2, depending on the direction of the change in CoG, the x-, y- or z-location should be used (Hibbeler, 2016).

$$\text{CoG} = \frac{\sum(\text{Mass} \cdot \text{Location})}{\sum \text{Mass}} \tag{4.2}$$

This calculation provides a preliminary estimation based on the weight of the VentoFoils. However, after the force calculation of the VentoFoils the weight of the foundations is added and a new warning can be given. The way the weight of the foundation is calculated is described below.

Scenario, as calculated by lightweight calculation	Update of Stability Information
Lightweight change $>$ 2%	Yes, using new incline result
LCG change $>$ 1% of L (either forward or aft)	Yes, using new incline result
VCG change $>$ 1%	Yes, using new incline result
1% $<$ Lightweight change $\leq$ 2%	Yes, using lightweight calculation
0.5% of L $<$ LCG change $\leq$ 1% of L (either forward or aft)	Yes, using lightweight calculation
0.5% $<$ VCG change $\leq$ 1%	Yes, using lightweight calculation
Lightweight change $\leq$ 1%	No
LCG change $\leq$ 0.5% of L (either forward or aft)	No
VCG change $\leq$ 0.5%	No

Table 4.1: Required Update of Stability Information based on Changes (IMO, 2024)

There are three standard foundations used by Econowind when placing a VentoFoil on the deck, which can be customised based on height or configuration. Three real-life examples of the foundations are shown in figure 4.6. The first foundation often results in a complex construction with diagonal bracing, and its design is highly dependent on the height of the foundation. The second foundation is not scalable to large heights, since H-profiles are available up to 1000 mm (IDL metals, 2024). The third foundation is a type of foundation building that can also house the VentoFoil's technology.

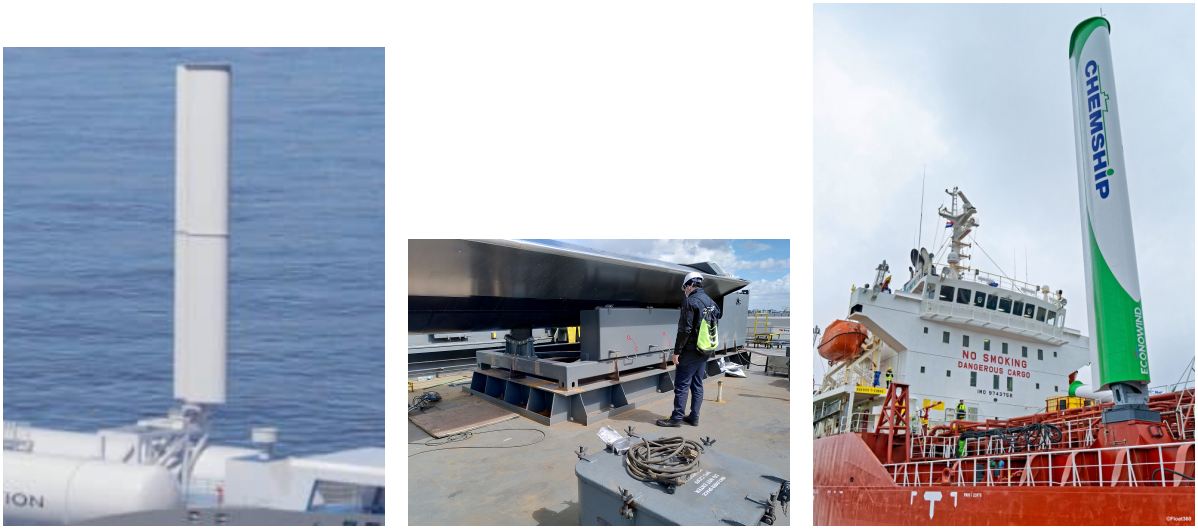

(a) Foundation 1 (Terntank, 2024) **(b)** Foundation 2 (Econowind, 2024) **(c)** Foundation 3 (SWZ Maritime, 2024)

Figure 4.6: Possible foundations for VentoFoil placement on deck.

In the model, the third foundation is simplified to estimate the weight of the foundation. This simplification assumes all walls to be vertical and the door is not included in the calculation. As this is a significant assumption, a safety factor is applied. The structural calculations (as shown below) are basic calculations and make it possible to estimate the weight. The results are validated with existing structural engineered foundations and their dimensions.

The simplified version of foundation 3 has to be strong enough for the gravity force of the VentoFoil and the moment due to the resultant force at the highest possible apparent windspeed. For both the force and the moment, calculations are performed to check whether the column as a whole is strong enough and whether the plates within the column will not buckle under the load.

Equations 4.3 and 4.4 are for the critical force of the column and the separate plates respectively. In figure 4.7 the dimensions used in the equations are given in a sketch. The column is made from steel with an elasticity modulus of $E = 210GPa$ and a Poisson's ratio of $\nu = 0.3$. The buckling coefficient and the bending stiffness of the plate can be calculated with equation 4.5 and 4.6 respectively.

$$(P_{cr})_{column} = \pi^2 E \frac{I}{l^2} = \frac{2\pi^2 E}{3} \frac{hb^3}{l^2} \tag{4.3}$$

$$(P_{cr})_{plate} = \frac{k_c \pi^2 D}{b} \tag{4.4}$$

$$k_c = \left(\frac{mb}{a} + \frac{a}{mb} \right)^2 \tag{4.5}$$

$$D = \frac{Et^3}{12(1-\nu^2)} \tag{4.6}$$

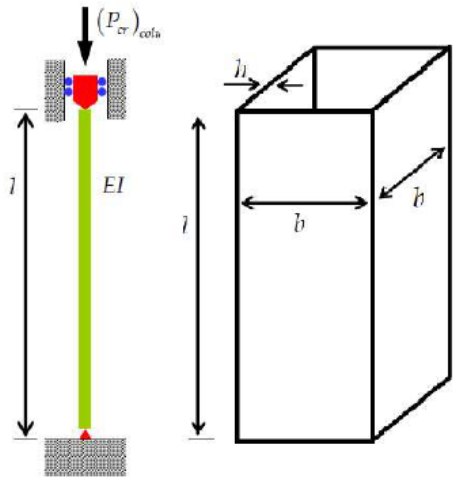

Figure 4.7: Definitions for the critical strength calculation of a column.

To find the critical stress in the column and the plate, equations 4.7 and 4.8 are used. The moment used for these calculations is the maximum resultant force multiplied by the arm length for each slice of the VentoFoil.

$$(\sigma_{cr})_{column} = \frac{Mh}{I} \tag{4.7}$$

$$(\sigma_{cr})_{plate} = \frac{k \cdot \pi^2 \cdot D}{s^2 \cdot h} \tag{4.8}$$

If the critical stress for the plate is the most important factor, both the thickness and the number of stiffeners can be varied in the model. The result of the calculations is the thickness, number of stiffeners and thus the weight of the foundation.

4.2.2. Regulations: Navigational Brigde Visibility

In the IMO regulation on 'Navigational Bridge Visibility' (2024) defines the maximal blind sectors, viewed from the conning position. In figure 4.8 a visualization of these regulations is shown. Within a $10°$ angle from the bow, the blind sector should be a maximum of $5°$, outside this zone, the blind sector is allowed to be a maximum of $10°$. The total arc of blind sectors shall not exceed $20°$. The clear sectors between blind sectors shall be at least $5°$.

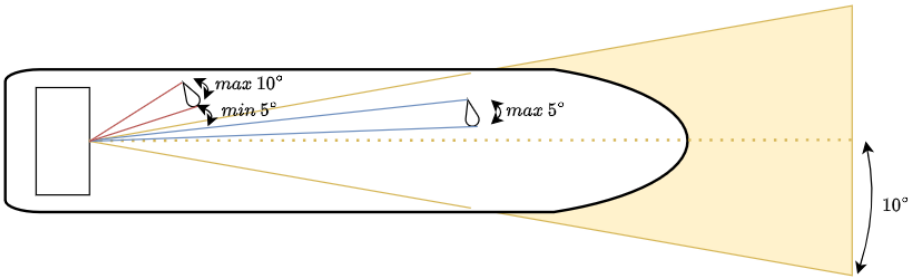

Figure 4.8: Navigational Bridge Visibility

This regulation is implemented in the model as a warning message, the warning includes which angle is too small or too big. The model considers the angles at which the VentoFoils are turned perpendicular to the view from the conning position.

4.3. Force Balance (Baseline- and VentoFoil calculations)

The Force Balance includes the following forces on the vessel: resistance, thrust, rudder force, and wind forces on the VentoFoils and the deckhouse. The wind forces on the deckhouse are described in section 4.3.1, while the interaction effects are covered in section 4.3.2. The resistance, thrust, and rudder force calculations are detailed in section 4.3.6. The forces on the VentoFoils are calculated as explained for the existing Econowind model in section 3.1.11.

4.3.1. Deckhouse

In the baseline calculation, only the deckhouse is subjected to wind forces. As discussed in subsection 4.1.1, for every height element this calculation is made separately to vary the windspeed and angle over the height. The deckhouse is assumed to be box-shaped with a fixed length and breadth. In figure 4.9 the deckhouse is shown with its projected area. The wind force can be calculated with equations 4.9 and 4.10, in which the drag coefficient (C_d) is assumed to be 2.1 since this is the maximum value for C_d for square boxes under an angle (The Engineering ToolBox, 2004).

$$F = A_{projected} \cdot p \cdot C_d \tag{4.9}$$

$$p = \frac{1}{2}\rho \cdot V_a^2 \tag{4.10}$$

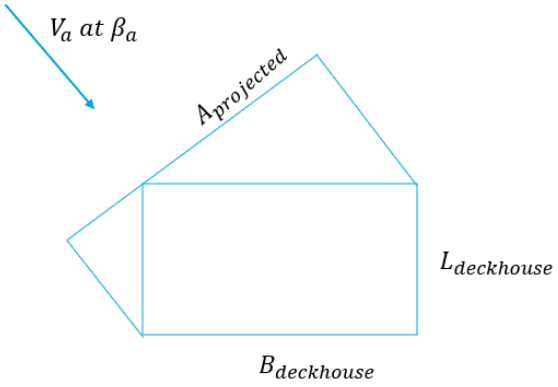

Figure 4.9: Topview of the deckhouse for wind force modelling

4.3.2. VentoFoil forces including Interaction

In this model, the VentoFoils are placed on deck, to give a more accurate prediction of the VentoFoil forces at specific wind speeds and wind angles. The interaction between the sails, the interaction between the deckhouse and the sails and the interaction between the deck and the sails are taken into account. The corresponding modelling is described in subsections 4.3.3, 4.3.4 and 4.3.5 respectively.

4.3.3. Sail-Sail Interaction

There are some theories for the interaction between sails for example the interaction of sails in sailing competitions from Marchaj (2003), however, the interaction between suction wing sails and specific VentoFoils has not been studied intensively yet. Borren studied the interaction between VentoFoils (2022) and the possibility of changing the angle of attack of both interacting VentoFoils to increase the lift. However, in practice, the VentoFoils all have their own wind measurement at the top of the foil, which automatically sets the angle of attack. The wind speed and direction are measured at the top of the VentoFoil. Therefore, it does not register changes in the angle of attack, as the highest elements are not influenced by interaction.

Downstream of a VentoFoil the wind angle changes due to the suction and the shape of the VentoFoil. Figure 4.10 shows the flow around a VentoFoil at an angle of attack of $24°$. In the figure it can be seen that the apparent wind angle is different if a VentoFoil would be placed in the wake of this VentoFoil. The flow around a suction wing should be the same for all wind speeds since the fan power is adjusted at different wind speeds. The apparent wind angle in this figure has changed from $24°$ upstream to $12°$ downstream of the VentoFoil.

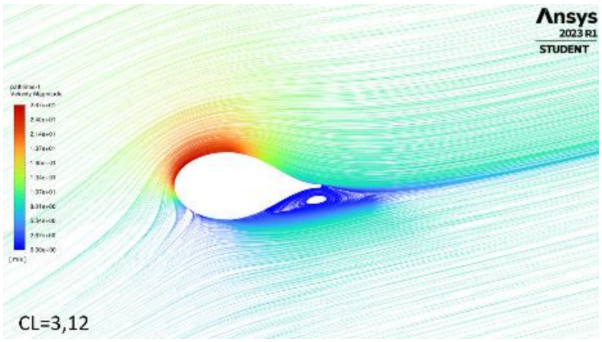

Figure 4.10: CFD of a VentoFoil at $AoA = 24°$ (de Gayffier, 2023)

The interaction, specifically the change in apparent wind angle change, depends on the distance at which the next VentoFoil would be placed. According to Marchaj (2003), the effect of an object like a sail can be experienced at a distance up to 10 times the height of the object. At high wind speeds, this distance is likely smaller (Simley et al., 2021). However, the exact pattern influence has not been investigated yet, so in the model, the influence region of 10 times the height of the VentoFoil is applied. This can be adjusted in the model after more research in CFD or wind tunnel tests are performed.

At a distance of 10 times the height of the VentoFoil, the wind conditions are the same as in the far-field. Within the influenced zone the change in angle is assumed to be linear. Although there might be some other correlation, it is not visible in the figure since the CFD cutout is too small.

In the ideal situation, the wind speed does not change in the downstream with respect to the upstream situation. However, this aspect of the VentoFoils has not yet been thoroughly studied. Since the research about the interaction of VentoFoils is still at an early stage, the interaction is modelled parametrised, so it can be adjusted after more research is performed. This parametrised modelling will be explained below.

The length of the influenced zone is defined as $10 \cdot s$ and at an angle between β_a and $\beta_a - 15°$. The apparent wind angle and the speed within this zone are adjusted based on the distance between the interacting VentoFoils using equation 4.11 and 4.12. The blue values can be adjusted after more accurate CFD results are available. This interaction is visually shown in figure 4.11 and 4.12. Here, it

can be seen that depending on the distance between the VentoFoils, the number of the influenced sail elements can be found.

$$\beta_{a,inter} = \beta_a - 12° \left(1 - \frac{L_{betweenfoils}}{10 \cdot s}\right) \tag{4.11}$$

$$U_{a,inter} = U_{a,\infty} - 0 \left(1 - U_{a,\infty} \cdot \frac{L_{betweenfoils}}{10 \cdot s}\right) \tag{4.12}$$

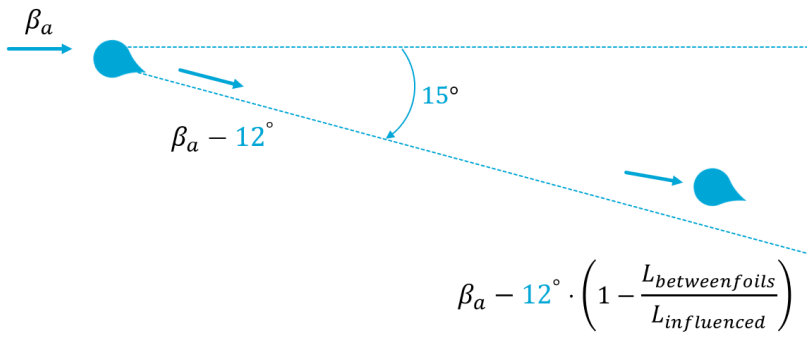

Figure 4.11: Interaction between VentoFoils shown visually.

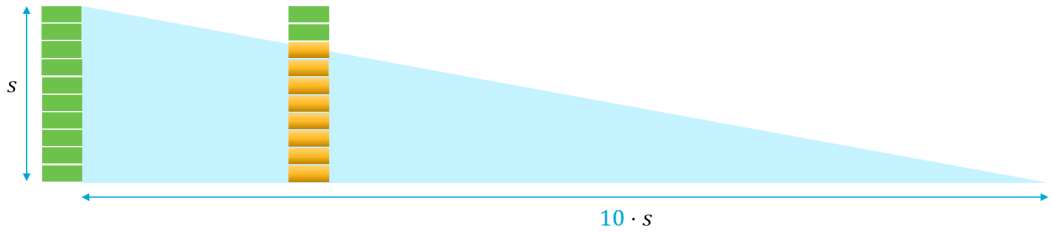

Figure 4.12: Interaction between VentoFoils shown in sideview.

The height of the influenced zone is assumed to be linearly at the distance of $10 \cdot s$. So in a triangle shape behind the first VentoFoil, the influenced VentoFoil experiences the difference in apparent wind angle and speed. In figure 4.14 an example is shown in which part of the VentoFoil performs at influenced angle and speed and part of the VentoFoil performs under normal wind conditions. Although the VentoFoils is interacting with another VentoFoil, the windmeter at the top of the VentoFoil experiences normal wind conditions, so the VentoFoil's angle of attack is not adjusted.

In the polar plot in figure 4.15 can be seen that VentoFoils placed next to each other are influneced under an apparent wind angle of 90° until 105°. At these angles the VentoFoil performs less efficiently, however, the forces are not zero.

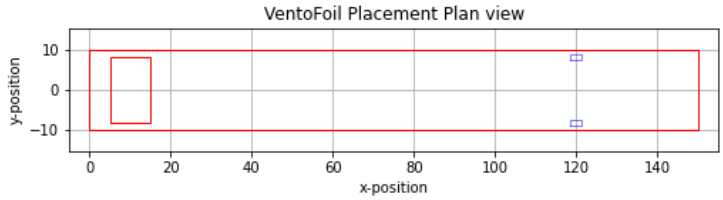

Figure 4.13: VentoFoil placement example resulting in the polar plot in figure 4.15.

The lift coefficient is added as a function depending on the Angle of Attack (AoA). The same method is used for the drag coefficient. When a VentoFoil is not interacting with another VentoFoil, the lift coefficient changes slightly over the height due to the wind gradient and therefore changes in the

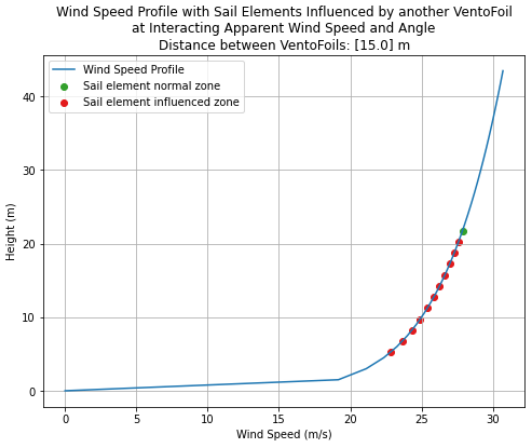

Figure 4.14: Sail elements with influenced height elements. The speed reduction in the influenced zone is assumed to be zero (following the line of the wind gradient).

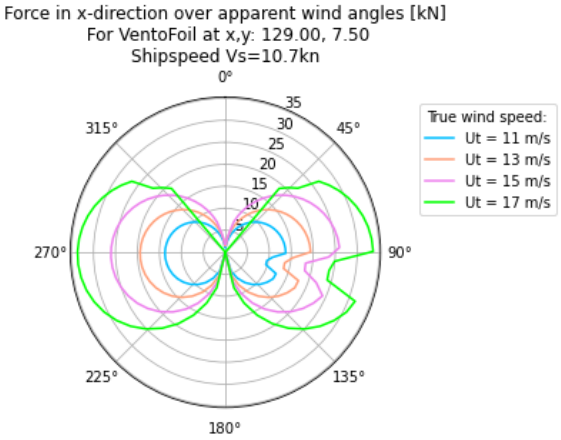

Figure 4.15: Polar plot of only the portside VentoFoil in figure 4.13 including interaction with another VentoFoil. The 16m VentoFoils are placed next to each other at a distance of 15m.

apparent wind angle over the height. With the interaction between VentoFoils, the apparent wind angle and therefore the angle of attack changes significantly as shown in figure 4.16.

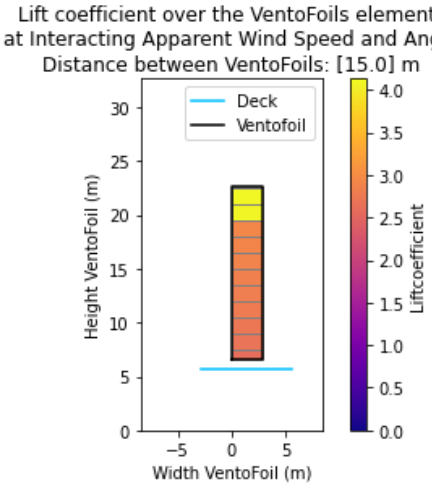

Figure 4.16: Lift coefficient change over sail height elements at influenced apparent wind angle and speed. The top 2 elements act at an AoA of 25°, and the elements below act at a lower AoA resulting in a lower lift coefficient.

Since the assumption is made that the speed reduction in the wake of a VentoFoil is zero, the influence of this assumption is tested in a sensitivity study. In figure 4.17, the results are plotted, showing the power reduction of two 30-meter VentoFoils placed next to each other at a distance of 10 m and 20 m. For this sensitivity study, an extreme case is selected, a small vessel with two 30-meter VentoFoils placed relatively close to each other. As can be seen in the figure the differences in power reduction in this case are noticeable but small. Therefore the assumption of zero speed reduction in the wake of a VentoFoil is justified. This sensitivity study however shows that if new research finds a speed reduction in the wake of a VentoFoil, it can be easily adjusted in the model.

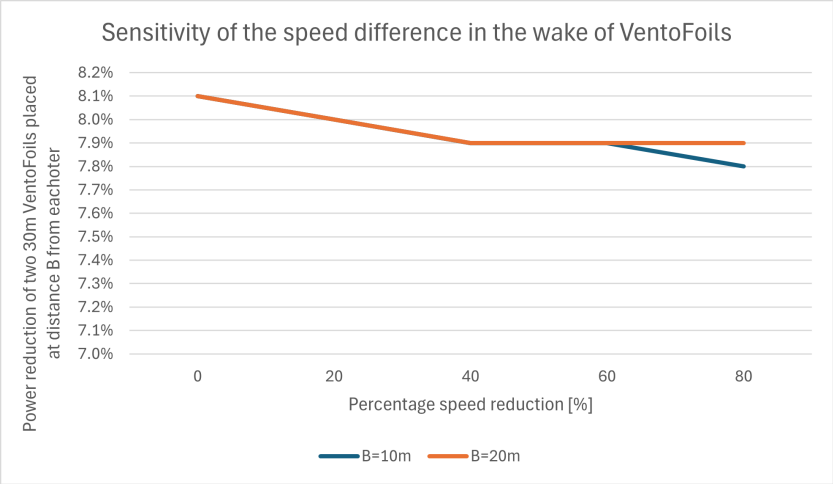

Figure 4.17: Sensitivity study on the influence of the speed decrease in the wake of a VentoFoil.

4.3.4. Deckhouse-Sail Interaction

If VentoFoils are placed close to the deckhouse, keeping in mind the visibility rules, this can have an impact on the forces and thus the polar plot. In figure 4.18, the top view of the modelled interaction is shown. The VentoFoil is assumed to be influenced in the rectangle shape downstream of the deckhouse. Within the influenced zone, the forces are assumed to be zero since the wake is turbulent and results in forces in all possible directions. The same way as for the sail-sail interaction is used for the height of the influenced zone: the length of the influenced zone is 10 times the height of the deckhouse and is triangle-shaped.

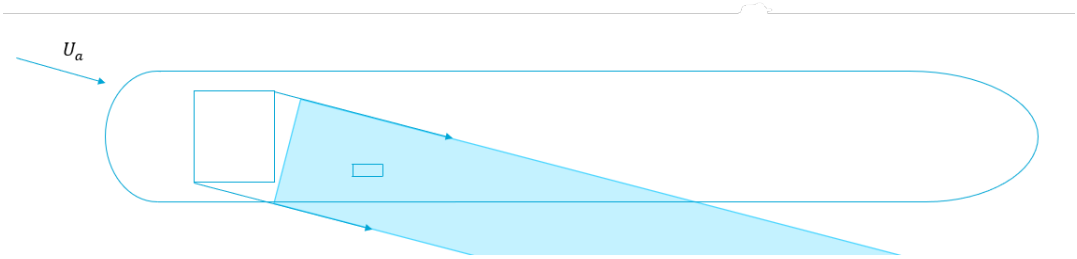

Figure 4.18: Deckhouse interaction top view

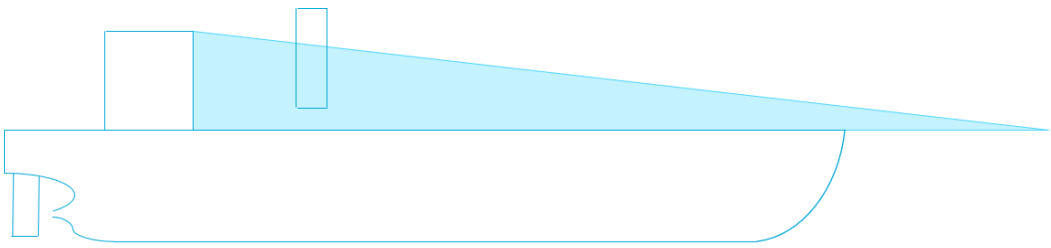

Figure 4.19: Deckhouse interaction side view

In a similar situation as sketched in figures 4.18 and 4.19 the sail elements are divided into normal operating sail elements and deckhouse zone elements, meaning the forces are zero at those sail elements. This is shown in figure 4.20 and visible in the polar plot in figure 4.21.

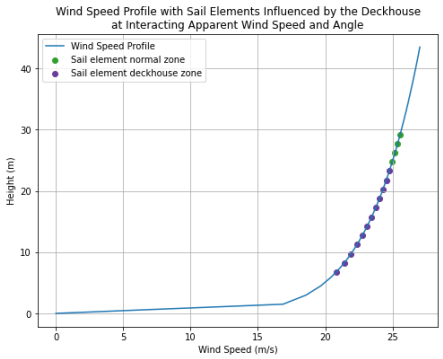

Figure 4.20: Sail elements with Interaction with the deckhouse

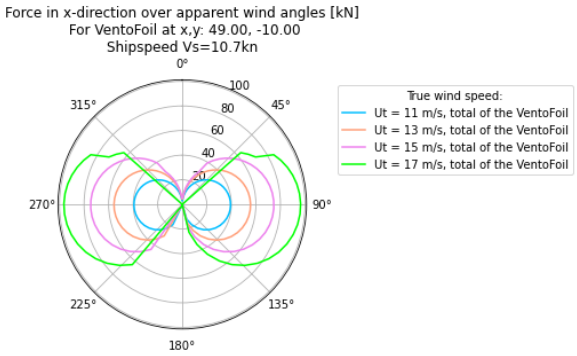

Figure 4.21: Polar plot including deckhouse interaction

4.3.5. Deck-Sail Interaction

The vessel's deck acts like a flat plate placed in the wind, creating a boundary layer separation. Most of the boundary layer is turbulent, meaning the forces on the VentoFoil are hard to predict and can be in every direction, therefore the forces within the turbulent layer are assumed to be negligible (same principle as for the deckhouse interaction). In figure 4.22 the phenomenon of boundary layer separation is shown, including its parameters. The height of the separation layer depends on the distance over which the wind has already travelled since the first touch of the deck (x_{sep}). This distance is calculated assuming a rectangle deck ($L \cdot B$). At distance x_{sep} the Reynolds number can be calculated using equation 4.13. The laminar zone occurs at low Reynolds numbers (up to $5 \cdot 10^5$), followed by the transition zone at somewhat higher Reynolds numbers ($5 \cdot 10^5$ - $3 \cdot 10^6$), and beyond that, the flow enters the turbulent region. The height of the laminar boundary layer (δ_{lam}) and the turbulent boundary layer (δ_{turb}) can be calculated with equations 4.14 and 4.15 respectively (Louisiana Tech University, n.d.).

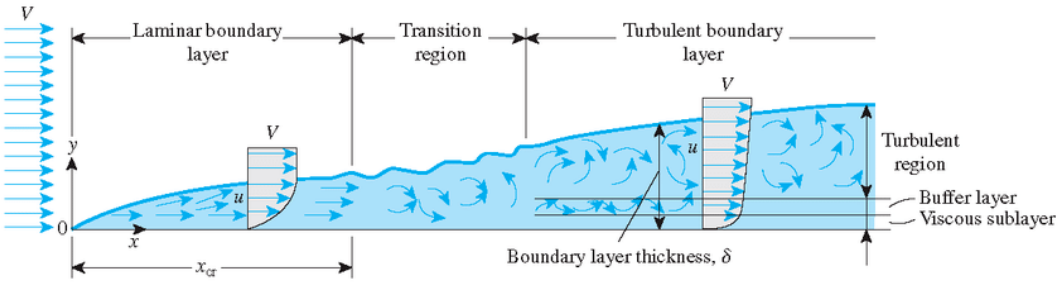

Figure 4.22: Separation layer (Houbraken, 2018, January)

$$Re_{x_{sep}} = \frac{\rho_{air} \cdot U_a \cdot x_{sep}}{\mu_{air}} \tag{4.13}$$

$$\delta_{lam} = \frac{5 \cdot x_{sep}}{\sqrt{Re_{x_{sep}}}} \tag{4.14}$$

$$\delta_{turb} = \frac{0.37 \cdot x_{sep}}{Re_{x_{sep}}^{1/5}} \tag{4.15}$$

Depending on the distance from the wind's first touch on the deck to the position of the VentoFoil, the lower height elements have neglectable forces, which is shown in figure 4.23.

Figure 4.23: Side view of the interaction between the deck and the VentoFoils.

4.3.6. Force and Moment equilibrium

After all forces on the vessel caused by the wind are calculated, a calculation of the thrust and rudder angle can be made. This is done by a force equilibrium in x- and y-direction and a moment equilibrium around the z-axis. In the normal operation case, the forces on the VentoFoils are left out.

First, the moment equilibrium around the z-axis (yaw-moment) is calculated to find the rudder forces. The moment equilibrium is shown in figure 4.24 and equation 4.16. However, in this equation, it is assumed that the hull resistance in the y-direction is acting on the Longitudinal Center of Gravity (LCG), which in practice is not the case.

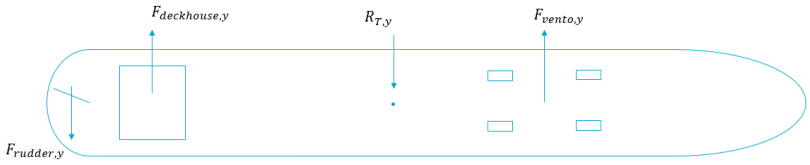

Figure 4.24: Momentequilibrium around the z-axis (including VentoFoils)

$$F_{rudder,y} \cdot (LCG - x_{rudder}) = F_{deckhouse,y}(LCG - x_{deckhouse}) - F_{vento_y} \cdot (x_{vento} - LCG) \tag{4.16}$$

The effect of the Center of Effort (CoE) of $R_{T,y}$ is tested and shown in figure 4.25. From this graph, it can be seen that the rudder angle is the largest if the VentoFoils are placed at the front of the vessel and the smallest when they are placed around the LCG. The angles are small ($< 0.025°$) and stay small for different CoEs of $R_{T,y}$. This means that the assumption for the model is valid.

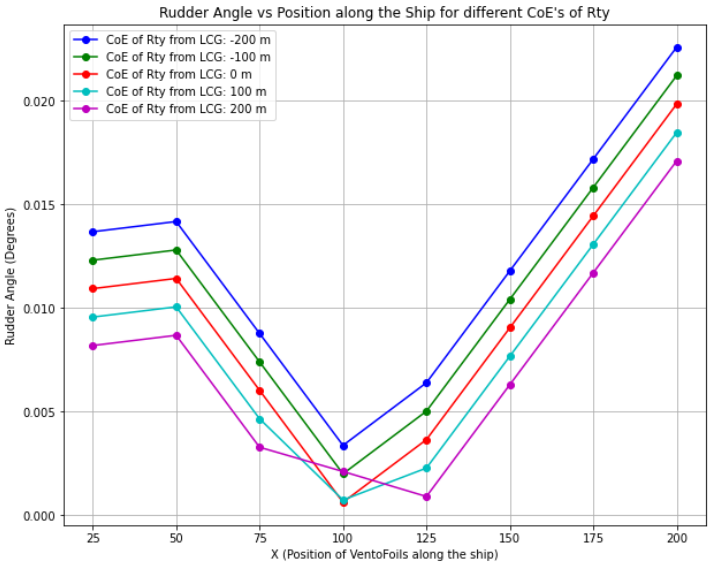

Figure 4.25: The effect of changing the CoE of $R_{T,y}$ on the rudder angle.

The rudder is assumed to have a surface of A_{rudder} that can be calculated with equation 4.17, with L, B and T being the dimensions of the vessel (Wärtsilä, 2024). The height of the rudder is assumed to be $H_{rudder} = 0.8 \cdot T$ and thus the length of the rudder is $L_{rudder} = \frac{A_{rudder}}{T_{rudder}}$.

$$A_{rudder} = L \cdot T \cdot 0.01 \cdot (1 + 25\frac{B}{L}^2) \tag{4.17}$$

The shape of the rudder is assumed to be a NACA0018 profile since it is a commonly used rudder profile and its lift and drag coefficients are known. The lift coefficient for angles of attack up to $25°$ is $C_L = 2\pi \cdot \alpha$ and the drag coefficient for low Reynolds numbers is $C_D = 0.0001\alpha^2 + 0.007$. The lift and the drag can be calculated with equations 4.18 and 4.19 respectively, resulting in the rudder forces in x- and y-direction as calculated in equation 4.20 and 4.21.

$$L = \frac{1}{2}\rho \cdot V_s^2 \cdot S \cdot C_L \tag{4.18}$$

$$D = \frac{1}{2}\rho \cdot V_s^2 \cdot S \cdot C_D \tag{4.19}$$

$$F_{rudder,x} = \sin(\alpha) \cdot L + \cos\alpha \cdot D \tag{4.20}$$

$$F_{rudder,y} = \cos(\alpha) \cdot L + \sin\alpha \cdot D \tag{4.21}$$

There is a force equilibrium in the x- and y-direction, meaning that the vessel is not accelerating in either direction. From that the thrust can be calculated using equation 4.22.

$$T = -(\vec{F}_{vento,x} + \vec{F}_{rudder,x} + \vec{F}_{deckhouse,x} - R_{T,x}) \tag{4.22}$$

For a given speed, the total ship resistance (R_T) can be found using equation 4.24 (Klein Woud and Stapersma, 2002). For vessels with a Froude number between 0.1 and 0.2, equation 4.25 yields. C_E is the specific resistance that can be found if the engine power, ship speed, and displacement in normal operation without VentoFoils are known (equation 4.26). With these equations all together and a known value for the force of the VentoFoils, it is possible to calculate the thrust force. The main vessel parameters required for this calculation are brake power (P_B), displacement (Δ), and ship speed (V_s), all in normal operation without VentoFoils.

$$R_T = (1 - t) \cdot T - F_{WAPS} \tag{4.23}$$

$$R_T = c_1 \cdot V_s^2 \tag{4.24}$$

$$c_1 = C_E \cdot \rho^{\frac{1}{3}} \cdot V_s^{\frac{2}{3}} \tag{4.25}$$

$$C_E = \frac{P_B}{\rho^{\frac{1}{3}} \cdot \Delta^{\frac{2}{3}} \cdot V_s^3} \tag{4.26}$$

To convert force to power, equation 4.27 can be used, however, it is only valid for the total power of the vessel (Hermans, 2024). The thrust force and the WAPS force should be added to find the total effective power (P_E) of the vessel. With simple proportional reasoning (equation 4.28 and 4.29), the effective engine power and the effective VentoFoil power can be found, respectively. To get from effective engine power ($P_{E,engine}$) to the brake power of the engine (P_B), multiple efficiencies are needed (η_H, η_O, η_R, η_S, η_{GB}, and η_e). Due to the low-fidelity level of the model, the matching procedure is not used to simplify the calculation process and reduce the number of required input parameters. From the baseline calculation, it is possible to find an overall efficiency to skip the matching step and all the separate efficiencies mentioned above. It is less accurate but estimates the proportions of the benefits for the different placement options and ship speeds.

$$P = F \cdot v \quad \longrightarrow \quad P_E = R_T \cdot v_s = ((1 - t) \cdot T - F_{WAPS}) \cdot v_s \tag{4.27}$$

$$P_{E,engine} = \frac{P_E \cdot (1-t)T}{(1-t)T + F_{vento}} \tag{4.28}$$

$$P_{E,vento} = \frac{P_E \cdot F_{vento}}{(1-t)T + F_{vento}} \tag{4.29}$$

With the calculated power for all wind directions and speeds, the probability matrix comes into play. The probability calculation is given in equation 4.30, where EX is the expected value. This method will be used to simplify the probability matrix of the resistance and thrust for the different wind speeds and angles to one value. The calculations for variance ($Var(X)$) and standard deviation (σ) are given in equation 4.31 and 4.32, respectively (Dekking et al., 2005).

$$EX = \sum_{x_k \epsilon R_x} x_k \cdot P_x(x_k) \tag{4.30}$$

$$Var(X) = E((X - E(X))^2) \tag{4.31}$$

$$\sigma = \sqrt{Var(X)} \tag{4.32}$$

The IMO wind probability matrix has a finite accuracy. The sum does not equal 1 due to rounding errors in the probability matrix. In probability theory, the change of all possible outcomes should be adding up to one (Dekking et al., 2005). Therefore the outcome is divided by the total chance of all possible outcomes together, being 0.996, to be able to give a fair power reduction.

4.4. Revenues and costs (Baseline- and VentoFoil calculations)

For a vessel sailing in normal operation, without VentoFoils, the main costs and revenues are the fuel costs and the cargo yield. Both values change after the VentoFoils are placed onboard. An explanation of the calculation of these costs and revenues is given below for the baseline calculation. Thereafter, their changes due to VentoFoil placement in fuel costs and cargo yield are explained. Last, a categorisation of the installation costs of the VentoFoils is described.

To determine the average fuel cost, the fuel type and its current/predicted fuel price p_{fuel} are inserted in the input screen. The fuel consumption can be calculated with equation 4.33 using the specific fuel consumption. The fuel cost is the fuel price times the fuel consumption (FC).

$$FC = sfc \cdot P_B \cdot t_{sailed/year} \tag{4.33}$$

The Cargo Yield (CY) of the vessel are the earnings from shipping freight. This is dependent on the distance that the cargo is transported and the type of cargo that is transported. In the model, the CY is calculated using the inserted average Freight Rate (FR) in $\$/MT$ with equation 4.34. The naval architect using the model can estimate the average freight rate based on the freight rates of the vessel in the past and the current freight rate predictions for the future. The model assumes an average utilization rate depending on the ship type shown in table 4.2.

$$CY = \#_{trips} \cdot DWT \cdot FR \tag{4.34}$$

At reference speed, part of the propulsive power comes from the VentoFoils reducing the fuel consumption. The cargo yield reduces only slightly caused by the weight addition of the VentoFoils. At reference power, the vessel has a higher speed at the same power. Therefore the fuel consumption remains the same. The cargo yield is calculated at the higher speed with a new rounded number of trips (equation 4.35).

$$\#_{trips,new} = V_{new} \cdot t_{sailed/year} \tag{4.35}$$

The total costs of the VentoFoils can be split into three categories: placement-dependent installation costs, fixed costs and costs dependent on the number of VentoFoils. All these costs are based on the experience of Econowind (Groot, 2024). Firstly, the placement-dependent installation costs are explained below.

Table 4.2: Average yearly utilization rate per ship type (IMO, 2009)

Ship Type	Average Yearly Capacity Utilization (%)
Containership	70%
Refrigerated Cargo Carrier	50%
General Cargo Ship	60%
Gas Carrier	48%
Combination Carrier	52%
Tanker	52%
Bulk Carrier	53%

- The steel costs of the foundation are $2000 per MT. The weight is calculated as explained in section 4.2.1.
- The cable costs are $50 per m. The distance of the cable from the deckhouse to the VentoFoil plus a margin of 20 m to reach the right place in the engine room is taken as the length of the cable.
- For the ducting, the same distance is used as for the cabling, with a price of $50 per m.
- The reference area, which consists of a 1-meter foundation and a 16-meter VentoFoil, has a known paint cost of $2000. The cost for painting the actual foundation and VentoFoil is scaled based on this reference area and price.

Secondly, the fixed costs independent of the size of the VentoFoils and the number of VentoFoils are defined below.

- Installation of control panels: $1000
- Class inspection: $4000
- Commissioning: $1000
- Logistics: $1000
- Project management: $1000
- Travel costs: $5000

Thirdly, the costs dependent on the number of VentoFoils are given below. The values given here are the costs per unit.

- Integration engineering of the VentoFoils on board: $500
- Lifting of the VentoFoils on board: $500
- Labour for installation: $2000
- Test and operation: $2000

Lastly, the cost of the VentoFoils themselves: A 16-meter VentoFoil costs around $250.000 and a 30-meter VentoFoil costs around $1.000.000.

4.5. Emission regulations (Baseline- and VentoFoil calculations)

For most ship owners, the Energy Efficiency Existing Ship Index (EEXI) is an important reason to decide on wind-assisted propulsion systems. For the EEXI reduction for WAPS (red box in equation 4.36), the polar plots including interaction effects are not relevant yet. However, this might change in the near future. The EEXI can be calculated with the potential polar plot of the VentoFoil at a constant wind speed over the height and without the interaction effects described in section 4.3.2. This part of the calculation is taken from the existing Econowind model as described in section 3.1.11.

The total EEXI formula is shown in equation 4.36 from IMO (2021), in which the red box is the WAPS part (equation 3.5). For EEXI the worldwide weather data from IMO is used. For the EEXI of the normal operation, the reference value for a specific vessel type is used since not all parameters in equation

4.36 are known.

$$
\begin{aligned}
EEXI = & \frac{\left(\prod_{j=1}^{n} f_j\right)\left(\sum_{i=1}^{nME} P_{ME(i)} \cdot C_{FME(i)} \cdot SFC_{ME(i)}\right) + (P_{AE} \cdot C_{FAE} \cdot SFC_{AE})}{f_i \cdot f_c \cdot f_l \cdot Capacity \cdot f_w \cdot V_{ref} \cdot f_m} \\
& + \frac{\left(\left(\prod_{j=1}^{n} f_j \cdot \sum_{i=1}^{nPTI} P_{PTI(i)} - \sum_{i=1}^{neff} f_{eff(i)} \cdot P_{AEeff(i)}\right) C_{FAE} \cdot SFC_{AE}\right)}{f_i \cdot f_c \cdot f_l \cdot Capacity \cdot f_w \cdot V_{ref} \cdot f_m} \\
& - \frac{\left(\sum_{i=1}^{neff} \boxed{f_{eff(i)} \cdot P_{eff(i)}} \cdot C_{FME} \cdot SFC_{ME}\right)}{f_i \cdot f_c \cdot f_l \cdot Capacity \cdot f_w \cdot V_{ref} \cdot f_m}
\end{aligned}
\tag{4.36}
$$

The reference value for the EEDI (or EEXI) can be calculated using the following standard formula: $EEDI = a \cdot DWT^{(-b)}$ (Polakis et al., 2019). The coefficients a and b depend on the shiptype. This is shown in figure 4.26.

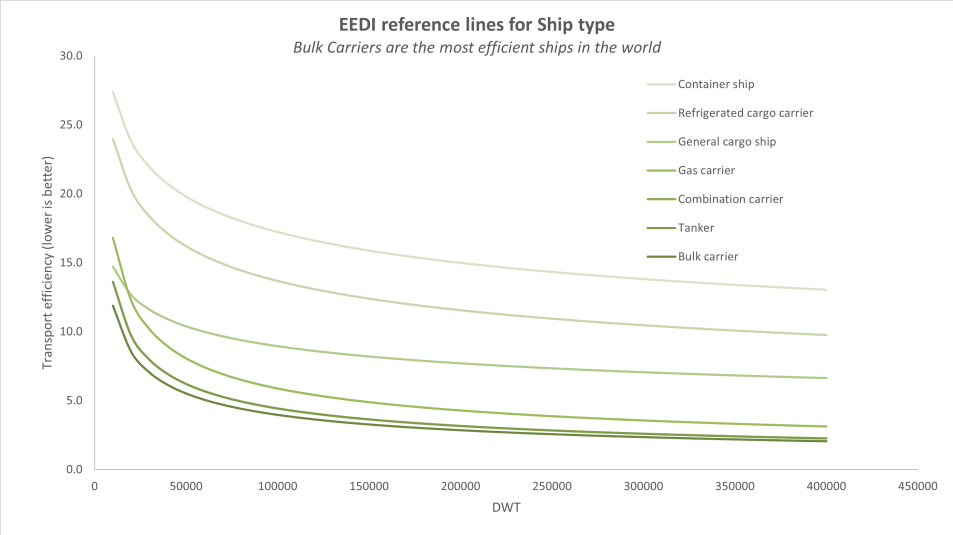

Figure 4.26: EEDI reference value per ship type (Groot, 2024)

The FuelEU Maritime regulations establish goals for reducing greenhouse gas (GHG) emissions that vessels must comply with. Equation 4.37 is used to calculate the GHG intensity of the energy used on board a ship. The calculation for well-to-tank (WtT) and tank-to-wake (TtW) can be found in the FuelEU regulations (The European Parliament and the Council of the European Union, 2023). For wind-assisted vessels, the reward factor (f_{wind}) is added, which has a value of 0.95 to 0.99 depending on the percentage of wind power used ($\frac{P_{wind}}{P_p}$).

$$
\text{GHG intensity} = f_{wind} \cdot (WtT + TtW) \tag{4.37}
$$

The Carbon Intensity Indicator (CII), is calculated with equation 4.38 and effectively rates a vessel based on the relative CO_2 emission. Every fuel type has a rule of thumb for CO_2 emission per metric ton of fuel used (Krantz, 2016). The CII of a vessel should improve every year from 2023 (with the reference year 2019), with a reduction of 2% every year (IMO, 2021).

$$
\text{CII} = \frac{\text{Annual total CO2 emissions}}{\text{Capacity} \cdot \text{Distance traveled}} \tag{4.38}
$$

4.6. Output

An example output for the normal operation, VentoFoil operation at reference speed and VentoFoil operation at reference power are given in figures 4.27, 4.28 and 4.29 respectively. The normal operation output makes it possible to see the differences in the revenues, costs and brake power.

The normal operation output (figure 4.27) consists of the expected power under wind conditions, including the wind forces on the deckhouse. This represents the brake power of the vessel, including the influence of the deckhouse. The brake power is higher than the initial input value because the hull resistance is assumed to be compensated for by the input brake power. However, the forces exerted by the wind on the deckhouses are added, leading to a higher expected power requirement. The EEXI is the reference value for the specific deadweight as described in section 4.5. The fuel costs and cargo yield are given per year.

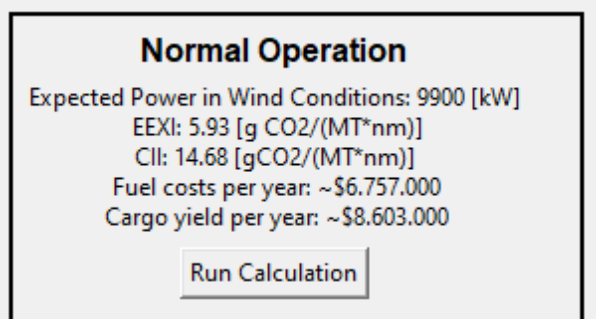

Figure 4.27: Normal operation output example

The output for the Ventofoils at reference speed (figure 4.28) shows a lower expected power since part of the power to sail at the reference speed is provided by the VentoFoils. The propulsive power generated by the VentoFoils is shown in the polar plot. In this case, it is visible in the plot due to the dip in the lines that two VentoFoils are interacting with each other. To get to the expected power the values in this polar plot are multiplied by the wind probability matrix. The difference in power compared with the normal operation is shown in percentages and as an absolute value, making it easier to compare. Next to the expected power, the standard deviation of the expected power is shown, the naval architect using the tool should decide on whether they want to have a placement option that performs well most of the time or performs very well once in a while in specific conditions. The weight of the VentoFoils including the foundation is shown, which is interesting since the height of the placement of the VentoFoils has a big impact on this value. The difference in weight also affects the cargo yield, as the vessel can carry less cargo. However, this raises the question of how much weight increase would cause the captain to adjust the cargo load. For this example vessel, with a cargo capacity (deadweight) of around 50,000 MT, a 14 MT difference would likely not impact the loading. The EEXI difference is shown in kW and in total EEXI change, this value is based on the ideal polar plot, without interactions. However, the height influence is not taken into account at EEXI, therefore, when placing the VentoFoils higher, this will not generate a higher EEXI reduction. The difference in fuel cost comes from the power reduction. The installation costs are the same for the reference speed and reference power situation since the placement and the VentoFoils are the same. It is helpful for the naval architect using this tool to have the placement-dependent installation costs presented separately, allowing them to vary the placement and immediately observe the changing costs.

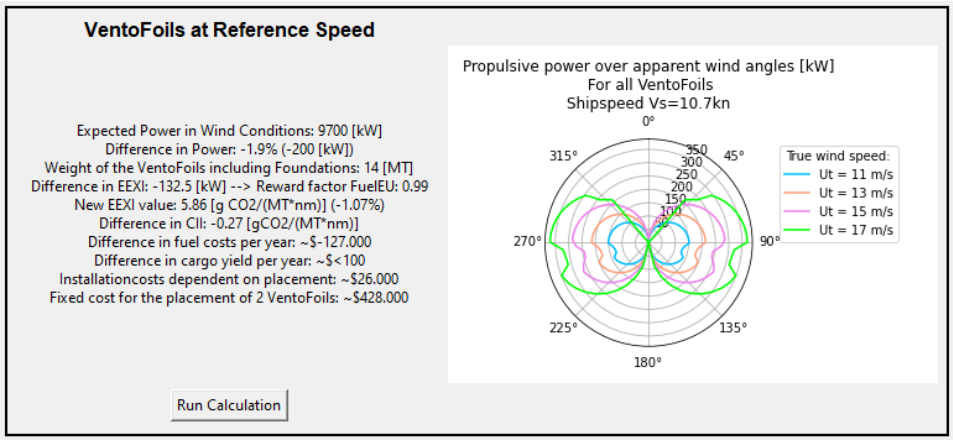

Figure 4.28: VentoFoils at reference speed output example

For the output of the operation with VentoFoils at reference power (figure 4.29), most of the values are comparable to the ones at reference speed, the differences will be explained. Since the vessel sails faster, at the same reference power but with the added propulsion power of the VentoFoils, the vessel sails faster, therefore the new speed is shown. The EEXI difference is compared to the reference EEXI of a vessel sailing at a higher speed. The difference in cargo yield comes from the higher number of trips sailed per year. If that is the case, the difference in cargo yield is quite high, making it an interesting option for shipowners. This way the naval architect using this tool can aim at a higher speed increase, resulting in higher cargo yields.

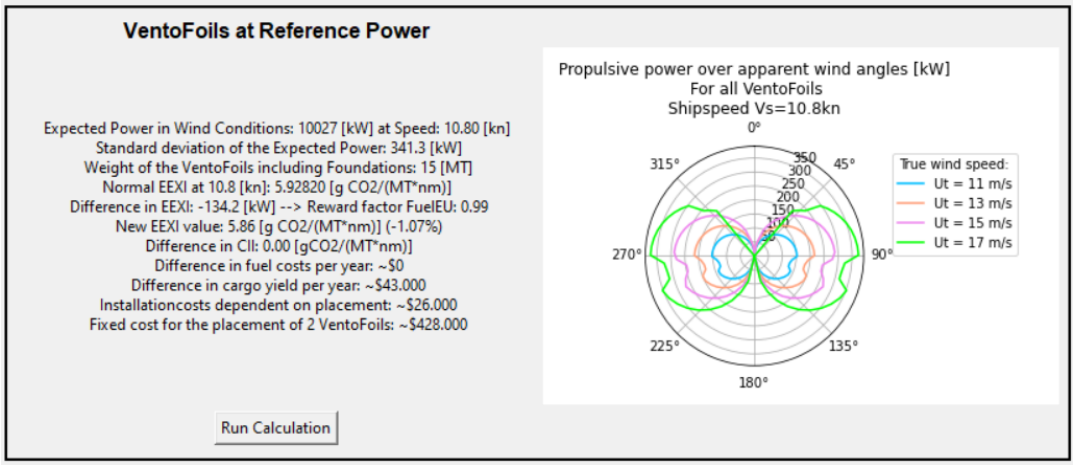

Figure 4.29: VentoFoils at reference power output example

The output provided by this software is distinct from existing models described in chapter 3. While force predictions for Wind-Assisted Propulsion System (WAPS) placements may not be directly unique, this tool enables designers to compare multiple placement options while considering interactions between sails, the deck, and the deckhouse. Additionally, it provides the capability to assess both the costs and benefits associated with each placement option, which makes it a comprehensive business case for customers.

While more advanced methods, such as CFD, can require significant computational time, this software is intentionally designed to be simpler and more efficient, providing designers with rapid feedback. It's a specialized tool for Econowind, helping to efficiently compare different VentoFoil placement options. Unlike digital twins, which are mainly used to simulate and monitor how a vessel performs during its operation, this tool helps designers make informed decisions about where to place VentoFoils. It evaluates both the aerodynamic interactions and the financial impact of each option, focusing on the design phase rather than ongoing use. This mix of performance analysis and cost-benefit review makes it a valuable tool for optimizing VentoFoil placement.

Current wind-assist models, like the ones described in section 3, primarily focus on vessel performance without addressing the financial considerations of different placements. This tool fills that gap by supporting designers not only to optimize aerodynamic efficiency but also to evaluate the economic differences between various placement options, ensuring a balanced consideration of both performance and cost.

The model does not prescribe the choices, it should be based on a user considering all changes presented in the model. The tool simplifies the decision-making process, also including errors if placement options are not possible due to regulations. The model does not include the general arrangement of the vessel, therefore the naval architect should still look at the possible placements on the vessel.

4.7. Conclusion

Based on this chapter it is possible to answer the third subquestion: *'How can an early-stage VentoFoil adoption decision-support model be developed to model the force balance of VentoFoil placement on a vessel under varying weather conditions, and assess their financial and environmental benefits?'*. The model described in this chapter shows a possible way of constructing an early-stage VentoFoil adoption model. In the model, the main vessel parameters, normal operation parameters and a possible placement option can be inserted. For a specific wind probability matrix, all the calculations are performed, making it possible to input a wind probability matrix from a certain navigational area. The model's calculations include the resistance of the hull, the rudder forces, the wind forces on the deckhouse and the VentoFoil forces. The VentoFoil forces are calculated considering the interaction effects of the deckhouse on the sail, of the VentoFoils with each other and the separation layer of the deck. Sailing with and without VentoFoils can be compared based on the financial and environmental results. Two VentoFoil cases are given, one sailing at reference speed, resulting in propulsive power reduction and the second at reference power, at a higher sailing speed. For these cases, the difference in environmental regulations (EEXI, CII and fuelEU) and the financial impact (installation costs, fuel costs reduction and cargo yield increase) are given. These results support the decision-making of the shipowner on whether to install VentoFoil on board and where to place them.

Reflecting on the requirements that were set in section 2.3, this VentoFoil Adoption model meets all three requirements. This model effectively supports the adoption decision, for possible selected placement options, comparing different scenarios for sailing with VentoFoils at reference speed or power. It is a low-fidelity model with short computational time, that does not require CFD calculations, but that still can estimate the interaction impact. And has an adaptable weather matrix.

5

Case study

A case study is performed to answer the following two subquestions: *SQ4: How do wind-assisting VentoFoils, or suction wings in general, influence the sailing speed, deadweight, and/or propulsion power of the vessel?* and *SQ5: What financial and environmental trends can be identified through the computational model for vessels equipped with VentoFoils for the different operational profiles?*. For the case study, the different placement options of 16 and 30-meter VentoFoils are compared. The VentoFoils are placed on an existing vessel, the Magritte (figure 5.1).

Figure 5.1: Magritte sailing with VentoFoils (The Maritime Executive, 2024).

The goal of this case study is to get insight into the different possibilities and general trends. Already in an early stage, the conclusion could be drawn that the specific placement does not have a big influence on VentoFoil performance as long as the VentoFoils do not interact. Therefore this difference is shown with option 3 and next to that interaction between VentoFoils is avoided.

The background information on this case study and the Magritte is given in section 5.1. Thereafter the selected placement options are given in section 5.2. In section 5.3, the results from the case study are shown, including sensitivity studies regarding fuel price and freight rate. From the results the conclusion is drawn in section 5.4, stepping in the position of the shipowner.

5.1. Case study background

The Magritte is currently sailing with two 16-meter VentoFoils in the configuration shown in figure 5.2. The vessel is a bulk carrier with hatches that slide to the side, so it is impossible to place VentoFoils there. The vessel is 32.34 meters wide, making it possible to place 30-meter VentoFoils on the vessel's sides. The VentoFoil cannot be placed in the middle because when folded down, the VentoFoil would stick out, and it can not be folded down above the hatchcovers. 16-meter VentoFoils can be placed either at the sides or in the middle. The basic vessel parameters and normal operation parameters are shown in table 5.1. The vessel is sailing all around the globe, therefore the worldwide weather matrix is used.

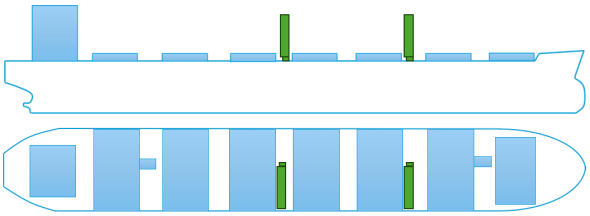

Figure 5.2: Current placement of the two 16-meter VentoFoils on board. In the top-view, the VentoFoils are tilted down. The hatches, two whiches and the deckhouse are marked in blue to show where the VentoFoils can not be placed. The VentoFoils are shown in green, the big square is the tilted VentoFoil and the small square is the foundation of the VentoFoil.

Table 5.1: Main vessel parameters Magritte

Basic Vessel Parameters	
Length [m]	228.99
Beam [m]	32.34
Scantling draft [m]	14.44
Depth [m]	20.20
X (begin and end) of the deckhouse [m]	11,29
Width Y of the deckhouse [m]	9.6
Height Z (above deck) of the deckhouse [m]	17.4
LCG (aft of midship) [m]	5
VCG [m]	10
Vesseltype	bulkcarrier

Normal Operation Parameters	
Reference Speed [knots]	10.7
Brake Power [kW]	9710
Number of trips per year	20
Sailing days per year	200
Distance sailing per year [nm]	51360
Deadweight [MT]	43013
Cargo Type	Bulk
Current Freight Rate [$/MT]	10
Fuel Type	HFO
Current Fuel Price [$/MT]	620

The options that were not selected as options could not be used because the model gave a warning for visibility or weight changes. The visibility warning is caused either because the angle of obstruction is too big or because the angle between VentoFoils is not large enough. The explanation of the visibility rules can be found in section 4.2.2. An example of an impossible placement option due to visibility is given in figure 5.3. In this example, the obstructed angle of both VentoFoils is overlapping and bigger than the allowed 5 degrees.

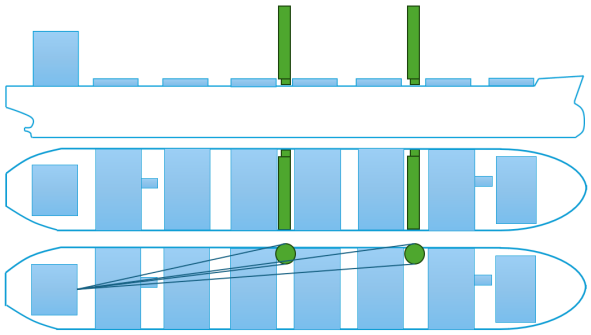

Figure 5.3: Impossible placement option due to visibility regulations. Two times the 30-meter VentoFoil.

Options where three or more 30-meter VentoFoils were placed on board, were non-favourable due to the large change in VCG. Depending on the percentage of VCG change, a new incline test has to be performed or new lightweight calculations have to be made. With three 30-meter VentoFoils at a height of 4m above the deck, the change in VCG is 0.6% and for four 30-meter VentoFoils, this is a change of 0.7%. Both are within the range of 0.5%-1% in which new lightweight calculations have to be made.

5.2. Placement options

A selection of 6 options was made to test the differences between multiple placement options of two 16-meter VentoFoils and find the difference between all other multiple numbers of 16 and 30-meter VentoFoils. After a selection was made for the following 6 options, options 1, 2 and 6 were tested for both the 16- and 30-meter VentoFoils, the others for only the 16-meter VentoFoils. If a placement option is not symmetric, it is only tested one way, since the model has symmetrical wind probability matrices, so it will result in the same power reduction, speed change and financial benefits. The 30-meter options are assymmetric since the VentoFoil cannot be placed in the middle because when folded down, the VentoFoil would stick out. Options 1-6 are shown graphically (figure 5.4 till 5.9). Thereafter the results will be shown in graphs with all these options together.

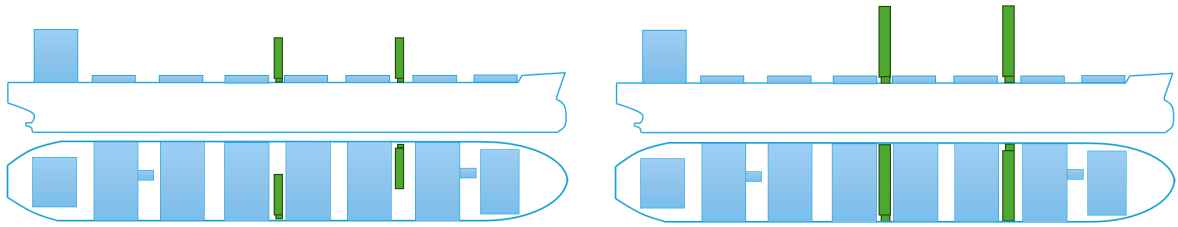

Figure 5.4: Placement option 1a, with two 16-meter VentoFoils and option 1b, with two 30-meter VentoFoils.

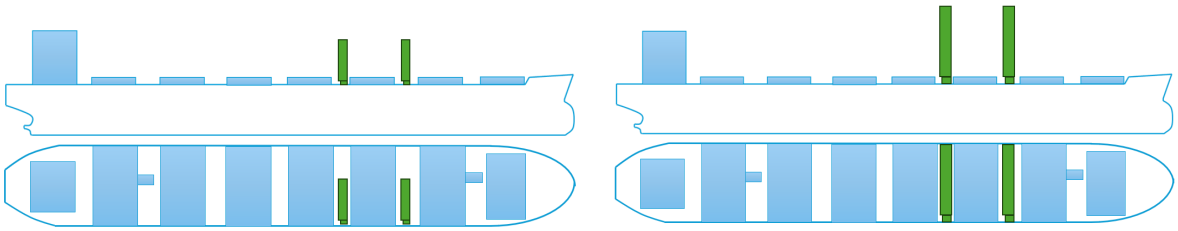

Figure 5.5: Placement option 2a, with two 16-meter VentoFoils and option 2b, with two 30-meter VentoFoils.

The third option (figure 5.6) was selected to show the influence of the interaction of the VentoFoils on the overall results. Onboard of the Magritte, this option was not possible for two 30m VentoFoils, since the space between the hatchcovers is too small for two times the cord of the 30m VentoFoil.

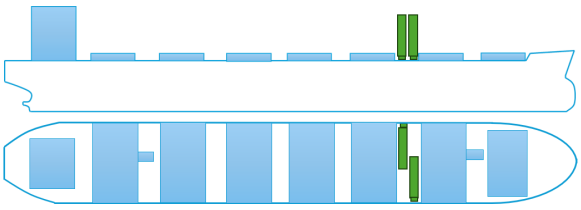

Figure 5.6: Placement option 3, with two 16-meter VentoFoils.

Next to the options of the placement of two VentoFoils, for the trendlines, it is important to compare them to the placement options with one, three or four VentoFoils.

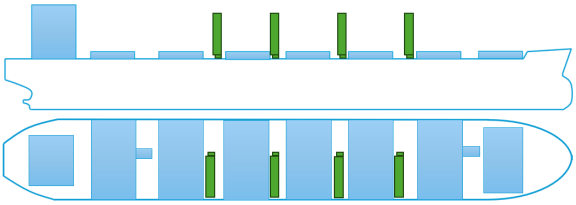

Figure 5.7: Placement option 4, with four 16-meter VentoFoils.

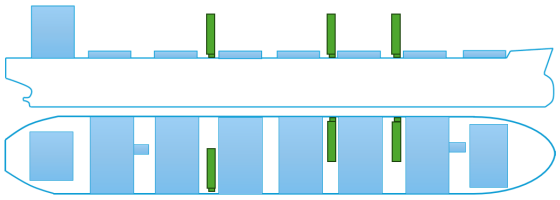

Figure 5.8: Placement option 5, with three 16-meter VentoFoils.

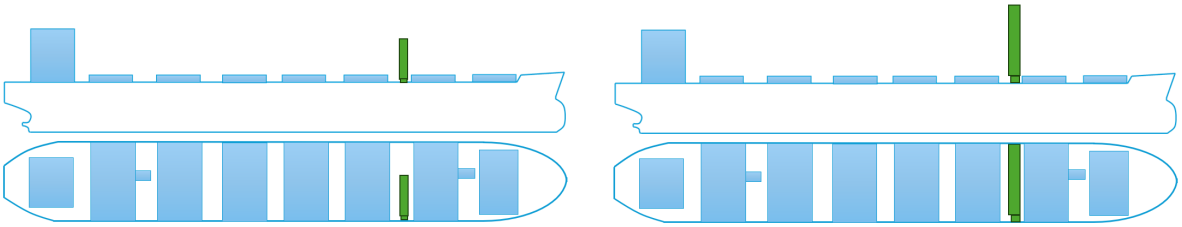

Figure 5.9: Placement option 6a, with one 16-meter VentoFoils and option 6b with one 30-meter VentoFoil.

5.3. Results

The following graphs compare different placement options for VentoFoils at various heights above the deck. At the end of this section, a list of considerations will be provided, based on the graphs and tables, to help decide whether to install VentoFoils and where the best placement would be for either 16-meter or 30-meter VentoFoils.

The weight addition of the VentoFoils including their foundations is shown in figure 5.10 and shows the difference between one, two, three and four 16-meter VentoFoils and one or two 30-meter VentoFoils. This weight addition is between -0.016% and -0.14% of the deadweight. Although the added weight represents only a small percentage of the vessel's overall weight, it is not within the margin of error.

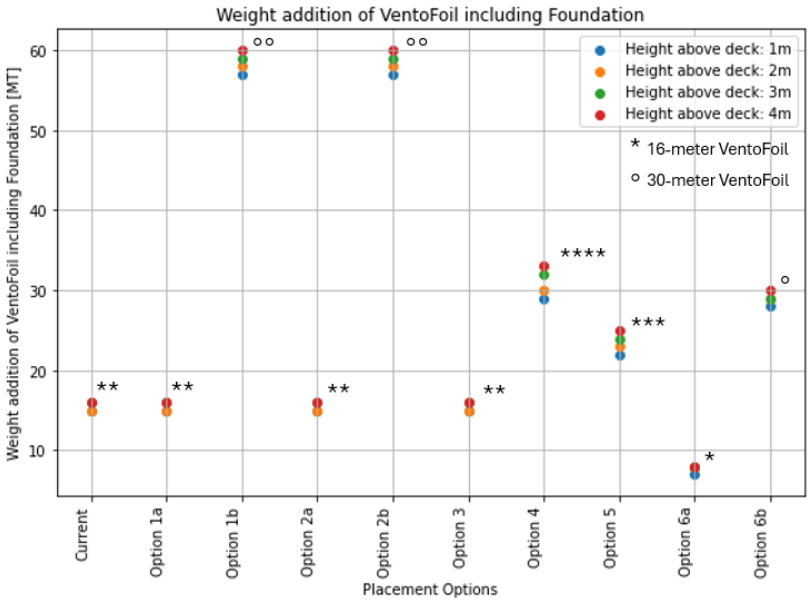

Figure 5.10: Weight addition of the VentoFoils including Foundation. The stars (*) indicate the number of 16-meter VentoFoils, where * = 1 VentoFoil, ** = 2 VentoFoils, *** = 3 VentoFoils, and **** = 4 VentoFoils. The circles (°) represent 30-meter VentoFoils.

The installation costs dependent on the placement are the costs of cabling and foundation. These costs can be varied by adjusting the placement of the VentoFoils higher or lower, or closer to or further from the engine room. These installation costs are shown for every placement option in figure 5.11. It can be seen that the foundation of the 30-meter VentoFoils is more expensive than the foundation of the 16-meter VentoFoil, since the forces are larger. However, the cabling costs are the same for both VentoFoil types. The height of the foundation changes these costs as can be seen in the different coloured dots. With respect to the total cost of VentoFoil placement, the differences between placement options and foundation heights are relatively small.

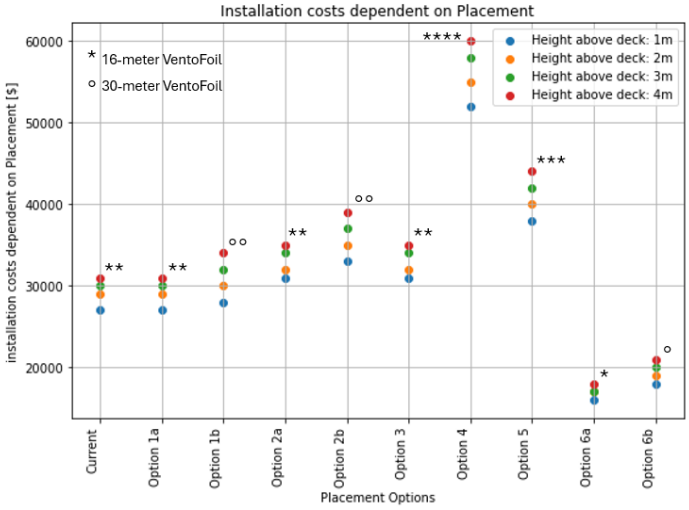

Figure 5.11: Installation costs dependent on the placement for the different placement options at a certain height above the deck.

The expected power reduction is shown in figure 5.12. The figure shows that a 30-meter VentoFoil creates a reduction comparable to approximately 3.5 16-meter VentoFoils. The lift and drag force scales with the wing's surface (equations 4.18 and 4.19), and the 30-meter VentoFoil has 3.3 times more surface than the 16-meter version. The highest reduction that can be expected on this vessel is around 2.3%, with two 30-meter VentoFoils.

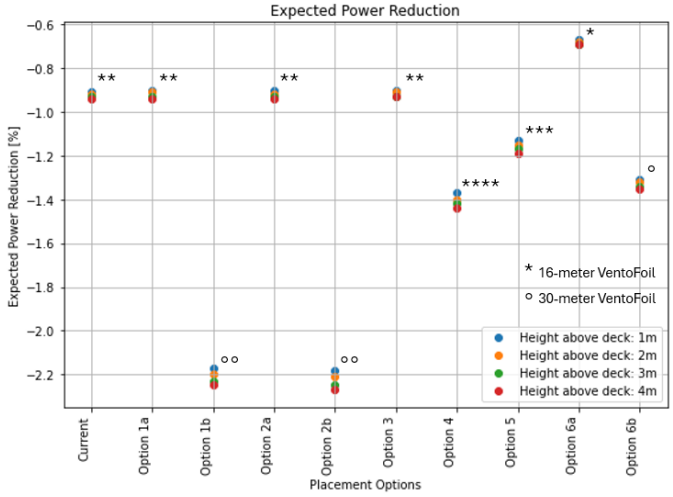

Figure 5.12: Expected power reduction percentage at reference speed for the different placement options at a certain height above the deck.

For a fuel price of 325, 525 and 725 $/MT, the expected power reduction (figure 5.12) will result in the fuel cost reduction shown in figure 5.13. These results are in line with the percentages of expected power reduction.

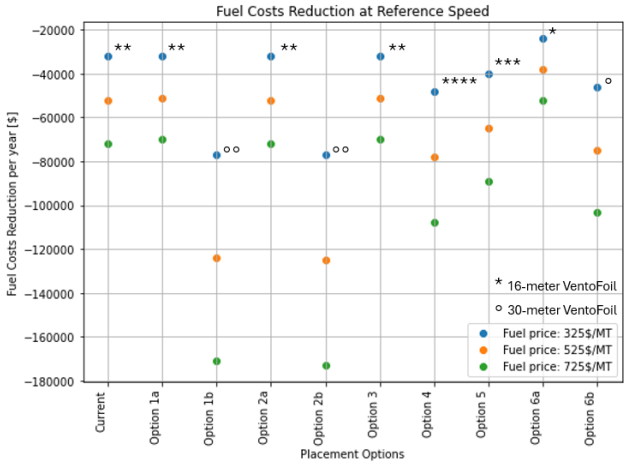

Figure 5.13: Fuel cost reduction at reference speed for the different placement options at a height of 1m above the deck for multiple fuel prices.

The speed increase at reference power is shown in figure 5.14. The model determines the average speed increase by increasing the sailing speed until the new expected power is higher or equal to the reference power. The accuracy of the speed increase can be adjusted. The accuracy in this case is 0.01 knots since from that point the reference power was within a margin of a maximum 8kW difference. For a higher accuracy, the model calculation would cost more time. The time scales linearly with accuracy. The duration can be limited by initially running the model with an accuracy of 0.1 knots to find the speed increase range. After identifying this range, the simulation can be rerun from 0.1 knots below the identified speed increase up to the maximum value, with an accuracy of 0.01 knots. This process can be repeated for more decimal places, improving accuracy step by step. However, from a certain point, the model might not be as accurate as the result anymore. The differences in forces are too small to notice the differences in speed increase within a margin of 0.01 knots, therefore only the height of 1 m above the deck is shown in the figure. The reference speed is 10.7 knots, meaning the speed increase is in the range of 0.28% and 1.77%. This will result in a cargo yield increase as shown in figure 5.15. A range of freight rates is shown in this figure. The higher the freight rate, the bigger the influence of the VentoFoils. The effect of these freight rates is also illustrated in the payback time (figure 5.17).

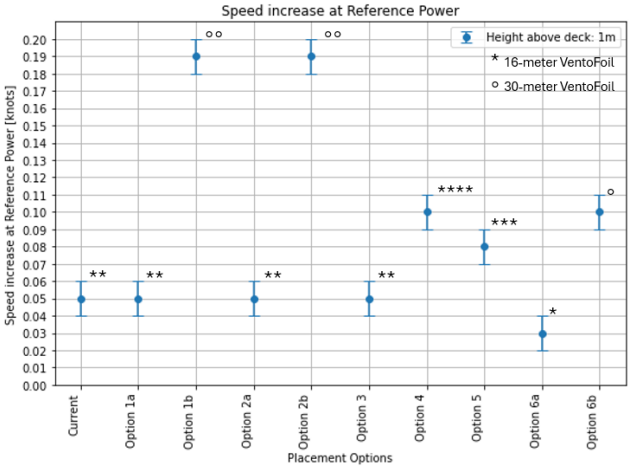

Figure 5.14: Speed increase at reference power for the different placement options at a height of 1m above the deck. The speed was increased with a stepsize of 0.01 knots, therefore the error bars were added.

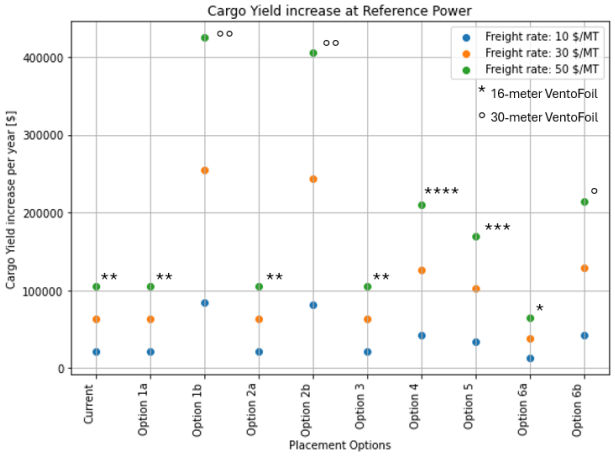

Figure 5.15: Cargo yield increase at reference power for the different placement options at a height of 1m above the deck at multiple freight rates.

The total costs of the placement of VentoFoils on board are shown in figure 5.16. These costs are compared with the yearly cargo yield increase at reference power or the yearly fuel consumption reduction to find the payback period. The payback period of the VentoFoils is shown in figure 5.17, in which is shown that the payback time at reference power is usually shorter than at reference power. However, this depends on the combination between freight rates and fuel prices. The differences are more obvious for the 30-meter placement options, however, from freight rates of 25$/MT the reference power case shows lower payback times for the 16-meter cases as well.

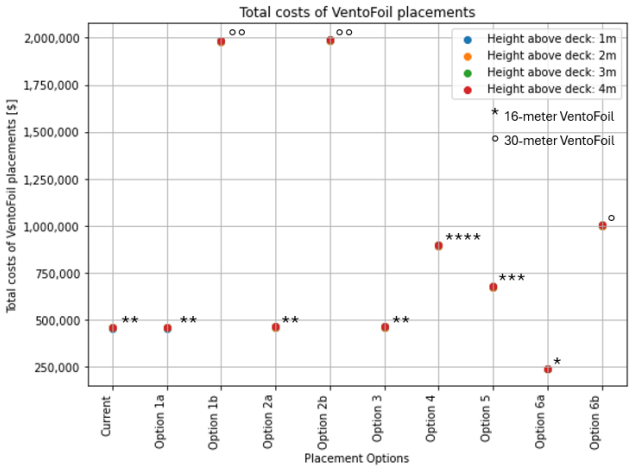

Figure 5.16: Total cost of the VentoFoils, including foundations, placement, engineering and transport (see section 4.4 for the whole cost division).

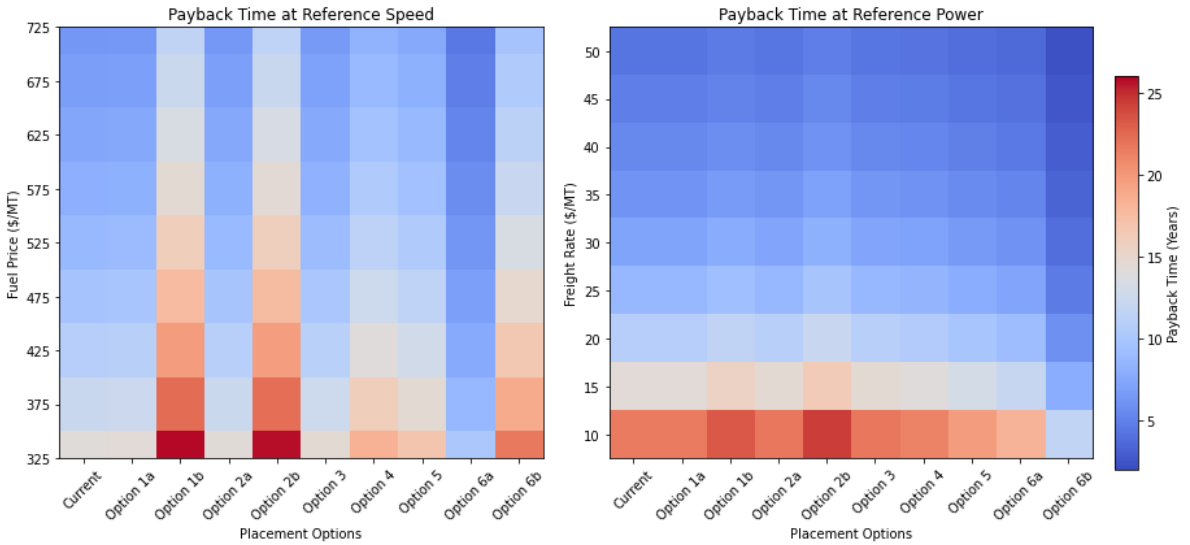

Figure 5.17: Payback time in the reference speed and reference power case for multiple fuel prices and freight rates.

The trend in power reduction, and thus fuel costs reduction, is shown in figure 5.18 for 16-meter VentoFoils and in figure 5.19 for 30-meter VentoFoils.

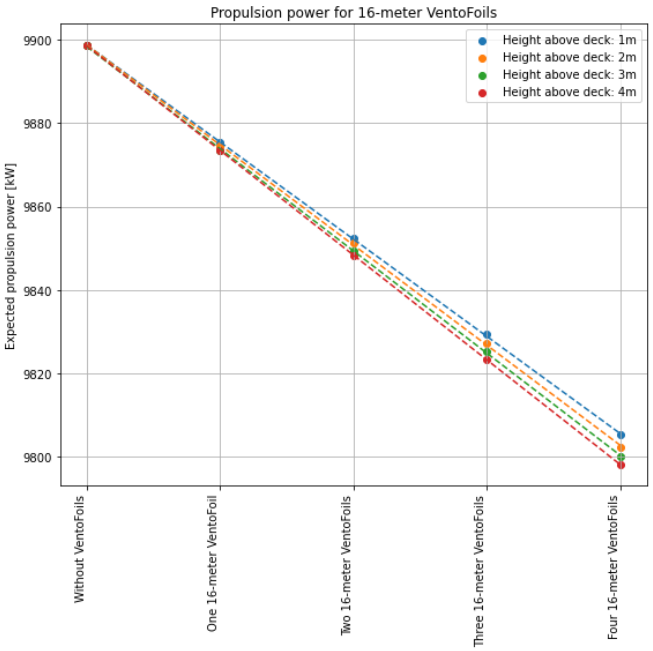

Figure 5.18: Trend in propulsion power for 16-meter VentoFoils

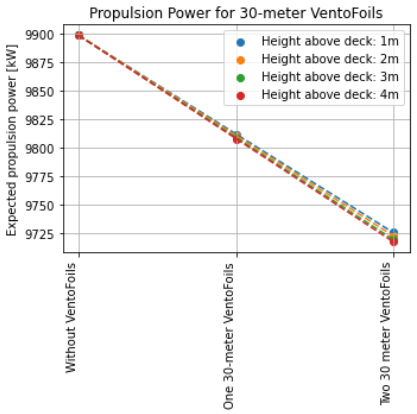

Figure 5.19: Trend in propulsion power for 30-meter VentoFoils

The financial trends when sailing at reference power at a higher speed can be seen in the speed increase (directly influencing the cargo yield). These trends are shown in figures 5.20 and figure 5.21. The differences in speed are quite small, therefore it can be discussed whether this will actually result in a higher number of trips or whether this difference will not be noticed.

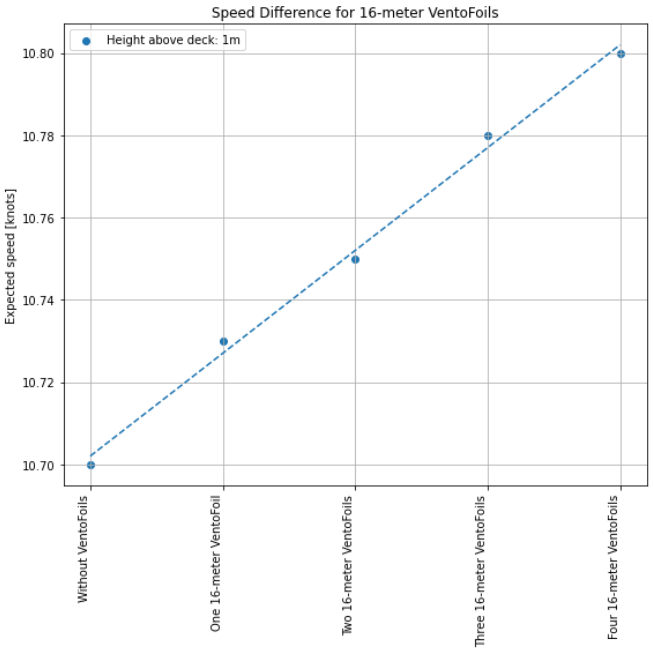

Figure 5.20: Trend in speed increase for 16-meter VentoFoils

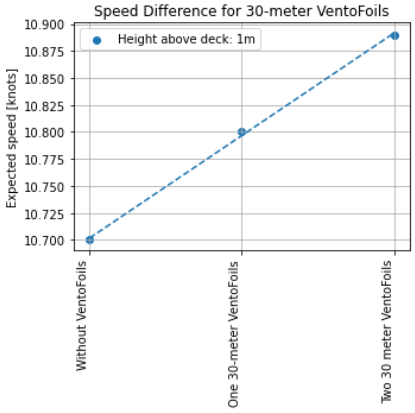

Figure 5.21: Trend in speed increase for 30-meter VentoFoils

5.4. Conclusion

This case study was performed to firstly test the functionalities of the model and considerations following from the results of the model. The goal of the model is to assist the engineer using the model in the VentoFoil adoption and placement decision. Since all the results are shown in different graphs, the following considerations will likely follow after seeing these graphs:

- It depends on what the shipowner's preference is: either to sail faster and sail more trips per year, which has an economical benefit in cargo yield increase or to sail at the same speed, but reducing the fuel costs. In both cases, the EEXI reduction is the same. The payback time of the VentoFoils is shorter at reference speed with the assumed freight rate and fuel price, possibly creating a preference for that option.
- The choice of how many VentoFoils to place on the deck can also be seen from an operational perspective. One 30-meter VentoFoil is similar to three to four 16-meter VentoFoils in the power reduction and speed increase. The consideration is then if the shipowner would like to save more space on the deck or would like to spread the forces. Three 16-meter VentoFoils offer more redundancy, however, they require separate maintenance checks. The total cost of one 30-meter VentoFoil is slightly more than that of four 16-meter VentoFoils (approximately 10%).
- The placement of a certain amount of VentoFoils in this case does not show big differences. However, the main conclusion is to place the VentoFoils (if possible) so that they do not interact with each other and the deckhouse. In most cases, they will not interact with the deckhouse due to the regulations on visibility, but the situation in which they interact with each other can in this case be avoided.
- It depends on the fuel price and freight rate whether it is more beneficial to sail faster or at the reference speed. However, in general, the payback time is often lower when sailing at a higher speed. This choice can be made depending on the freight rate and fuel price when sailing.

As a designer, I would progopse the ship owner to select two 30-meter VentoFoils (option 2b) on deck and operate at reference power to achieve a higher sailing speed. This setup has higher benefits for EEXI and increases the ship's speed, which is a strong selling point for customers. While this option has a slightly longer payback period compared to smaller, 16-meter VentoFoils, the long-term gains are significantly greater. Once the VentoFoils are paid off, they will deliver much higher efficiency and economic benefits than the 16-meter option.

Secondly, the case study helps to answer two of the subquestions. The first question that is answered within this case study is the following: *SQ4: How do wind-assisting VentoFoils (suction wings in general) influence the sailing speed, deadweight, and/or propulsion power of the vessel?* To begin with the influence of VentoFoils on the sailing speed. As shown in figure 5.14, the VentoFoils can increase the sailing speed when the average propulsion power is kept equal. These results depend on the amount of VentoFoils and the size of the VentoFoils, but the placement options researched within this case study show a speed increase of 0.75% to 2.35%. The deadweight changes with the weight of the VentoFoils including foundations, these are shown in figure 5.10. The weight addition is dependent on the span of the VentoFoil and the height of the foundation. For one or two 16-meter VentoFoils, the change in deadweight is almost unnoticeable compared to the total deadweight. In principle, this could result in a lower cargo weight. However, since the percentage is relatively small, the likelihood that this change will affect loading is minimal. The vessel is rarely fully loaded, and a difference of a few tons is usually not noticed or managed any differently. For the 30-meter VentoFoils or several 16-meter VentoFoils, the difference becomes bigger, resulting in a noticeable lower cargo capacity. Lastly, the effect of the placement of VentoFoils on the propulsion power of the vessel. The propulsion power is decreased in case the shipowner decides to keep on sailing at the speed but reduce the power. The power reduction is shown in figure 5.12, resulting in power savings up to 2.3%. These power savings are specific for this case study since there was no possibility of placing more VentoFoils on deck due to the visibility and stability regulations and the leftover space on deck between the hatch covers. For other vessels with more space on deck, a bigger lightweight or other center of gravity, the placement options might be less limited resulting in higher possible savings.

The second question answered within this case study is the following: *SQ5: What financial and environmental trends can be identified through the computational model for vessels equipped with VentoFoils for the different operational profiles?* The placement of multiple 16-meter VentoFoils follows a linear trend. For the 30-meter VentoFoils, a trend can not be identified, since there are not enough points. However, the same trend is expected for the 16-meter VentoFoils. In these graphs, placement options are plotted where as little as possible interaction effects occur. A possible trend when selecting interacting placement options is that as more VentoFoils are added to the deck, their impact reduces due to interaction effects. Beyond a certain number of VentoFoils, the power reduction might reach a saturation point, showing an asymptotic relationship. The same conclusion can be taken for the financial trend in speed difference and thus cargo yield, it shows a linear trend for both the 16-meter and 30-meter VentoFoils.

Since the EEXI is calculated assuming an ideal polar plot, without taking into account interaction effects, the EEXI reduction will always be a linear relation. Therefore the differences between placement options do not change the EEXI reduction. In the case of sailing at reference speed with VentoFoils, the fuel reduction becomes an environmental benefit as well.

6

Validation

Validating a design method is a crucial step to make sure that it produces reliable and practical results. By explaining the validation process used, this chapter answers the last subquestion: *SQ6: How can the predictions of the computational model regarding the influence of VentoFoils on a vessel be validated?* For the method used within the VentoFoil Adoption model, the Validity Square method was applied, which evaluates both the theoretical and empirical aspects of the model's structure and performance (Pedersen et al., 2000). The Validity Square method is useful because it allows researchers to systematically evaluate key aspects of the model's credibility and applicability in complex, real-world contexts. The validation process is divided into four parts: theoretical structural validity, empirical structural validity, empirical performance validity, and theoretical performance validity. Each section ensures that the model can be trusted to assist the VentoFoil adoption and placement decision. Each type of validity is discussed in detail below.

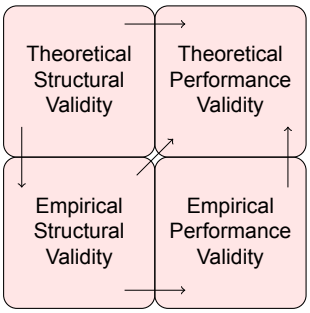

Figure 6.1: Validation square

6.1. Theoretical structural validity

In this research, the theoretical structural validity has already been addressed by selecting reliable sources for every assumption and equation used in the model. As a preparation for the model building, a literature review was conducted to ensure that all assumptions were supported by credible information. Additionally, the internal consistency of the model has been demonstrated through a flowchart (figure 4.1), which shows how the different parts of the model work together logically. This flowchart highlights how inputs and assumptions lead to appropriate outputs, supporting the overall reliability of the model. By carefully verifying each part of the model with trusted sources, the theoretical structural validity is confirmed as outlined in the Validation Square.

6.2. Empirical structural validity

For the empirical structural validity, the model was tested using sea trial data from an example vessel equipped with VentoFoils. The results are not exactly the same as the measurements from the sea trials, however, they are close. At reference speed, the model tends to produce conservative power reduction estimates that are 13kW lower. While at reference power, the speed increase predictions are slightly optimistic with a difference of 0.1 knots. Despite these small variations, the model reliably represents actual performance scenarios.

The financial validity can not be validated based on existing financial models mentioned in section 3.1.12 and 3.1.13, because the method used in this model is unknown and therefore the results can only be compared. However, the main results from the tools are the NPVs of suction wings, which is not a result of the VentoFoil Adoption Model. The CO_2 reduction found in the case study of the

Magritte in the current situation is approximately 10 times bigger than the CO_2 reduction seen in the Decision Support Tool (Kühne Logistics University, 2024). Since no method is available on this tool, it is impossible to tell where the difference comes from.

6.3. Empirical performance validity

The empirical performance validity tests whether the results from the model are useful to the ship owner and whether they will be able to make a VentoFoils adoption decision based on the results from the VentoFoil Adoption model. During the end phase of this master thesis, already several Econowind colleagues asked for results from the VentoFoil Adoption model for correspondence with possible customers. At the moment, the company has no other way of calculating some of the results, which would be very convenient for the sales department if they were accessible from the model.

The information from the model will give a first estimation of the ideal placement of VentoFoils on board in an early sales stage, providing a critical advantage in negotiations and decision-making. The fact that the calculation of possible placement options was requested for three potential customers during the thesis highlights the demand for this model and its relevance to Econowind's sales operations.

Additionally, as the Energy Efficiency Existing Ship Index (EEXI) regulations change, the model becomes even more relevant. The EEXI is now calculated by the theoretical performance of the VentoFoils without considering interaction and height variations. However, the regulations are changing to the obligation to consider those effects for the EEXI calculation. This model provides the possibility to calculate the EEXI based on more realistic polar plots, including the interaction between VentoFoils, with the deckhouse and the separation layer of the deck.

6.4. Theoretical performance validity

The theoretical performance validity is a theoretical check on whether the model will perform in different scenarios than performed in the case study. While the model performs well for a variety of vessels and placement configurations, it has limitations in extreme conditions, such as on very small vessels where the VentoFoils' forces significantly affect propulsion. Additionally, the model does not account for obstacles on deck despite the deckhouse, which could influence VentoFoil's performance. Therefore, while the model is theoretically valid for many scenarios, its use is not recommended for vessels with specific obstacles or extreme configurations.

6.5. Conclusion

The subquestion *SQ6: How can the predictions of the computational model regarding the influence of VentoFoils on a vessel be validated?* is addressed through the Validity Square method. The model's predictions are validated by ensuring theoretical structural accuracy by using reliable sources for its assumptions and equations, and by comparing the model's output with real-world sea trial data. This process showed that the model's predictions closely align with actual data. Additionally, the model's practical use is demonstrated, however, it does have limitations in extreme scenarios, such as for small vessels or vessels with obstacles on deck.

7

Conclusion

In this report, the goal was to show the impact of VentoFoil placement on a vessel from a ship owner's perspective to answer the main research question: 'What is the impact of VentoFoil placement on ships from a ship owner's perspective?'. A VentoFoil Adoption Model was created to find the financial and environmental impact of VentoFoil placement on board a vessel. Literature research investigated existing models on WAPS performance, decision-making or financial benefits. However, the models did not comply with all the set requirements. Therefore, the model created within this thesis aims to answer the research question by using the method described below.

The VentoFoil Adoption model first calculates the baseline, the vessel sailing without VentoFoils. This baseline calculation includes a vessel with the wind force on the deckhouse, the resistance of the hull and the rudder forces required for course stability. The wind is modelled with a gradient to provide an accurate estimation of wind conditions at specific height elements. After the calculation, the results are weighted by their probabilities using the wind probability matrix.

Secondly, the calculations of the vessel with VentoFoils are made. The model first checks whether VentoFoils can be placed at the selected location, using the regulations for visibility and intact stability. Then the forces on the VentoFoils are calculated, assuming interactions with the deck, between the VentoFoils and with the deckhouse. The interaction between VentoFoils is modelled in a simplified way assuming a change in the angle of attack in the wake of VentoFoil, but keeping the wind speed the same. The interaction with the deck is modelled as the boundary separation layer and will result in turbulence close to the deck. Lastly, the effect of the deckhouse on the VentoFoils is also creating a turbulent zone, in a triangled shape behind the deckhouse. When placed in such a turbulent zone, the VentoFoil is unable to generate a resulting force. With the forces of the VentoFoils, it is possible to find a new force balance. This results in an expected value, including the probability of windspeeds and angles, for the power at the same speed as the baseline calculations. So, it gives the propulsion power reduction that can be obtained if VentoFoils provide part of the power.

To determine the speed increase if the power is kept the same as in the baseline calculations, the same calculation is performed while iteratively increasing the speed. The iteration is stopped if the expected value for power is the same or higher than the reference power. This means that the average brake power usage of the vessel is the same as in the baseline conditions, however, in real life, the power would always stay the same and depending on the wind conditions the speed would increase.

For all three calculations, the baseline, the VentoFoil operation at reference speed and the VentoFoil operation at reference power, the costs of the VentoFoil placement, the fuel consumption and cargo yield are given. Next to that, the environmental benefits are listed, such as the reduction in Energy Efficiency Existing Ship Index (EEXI), the reduction of the Carbon Intensity Indicator (CII) and the reward factor in the FuelEU regulations. This gives the possibility to compare placement options based on their financial and environmental benefits, enabling a well-considered decision-making process.

Reflecting on the requirements that were set in section 2.3, this VentoFoil Adoption model meets

all three requirements. This model effectively supports the adoption decision, for possible selected placement options, comparing different scenarios for sailing with VentoFoils at reference speed or power. It is a low-fidelity model, that does not require CFD calculations. However, can estimate the interaction impact. Lastly, the model has an adaptable weather matrix.

A case study was performed to determine the influence of VentoFoil placement on the speed, dead-weight and propulsive power of the vessel. In this study, an existing bulk carrier sailing with two VentoFoils was used to verify the impact of various placement options. The weight estimation from the model indicates that on this vessel the placement of a maximum of either four 16-meter VentoFoils or two 30-meter VentoFoils is possible, due to visibility and intact stability limitations. With these numbers, the weight of the VentoFoil including the foundation increases the lightweight with 0.01% to 0.07%. The speed increase is in the range of 0.28% and 1.77%. Depending on the freight rate and the fuel price the choice can be made between sailing at reference speed or reference power. At most freight rates and fuel prices, it is more beneficial to sail at a higher speed, although the speed increases are relatively small. Whether or not the speed increase is noticeable in operation is open for debate. The trends found in the power reduction and speed increase are linear with the number of VentoFoils. However, this is the case for non-interacting VentoFoils. When more VentoFoils are placed on the deck and they interact with each other, a maximum (asymptote) will be probably reached.

This model was validated using sea trial data of an existing vessel, resulting in a relatively close match with the model's results. The empirical performance validity is proved by colleagues at Econowind, who also identified the convincing power of using the VentoFoil Adoption Model in sales.

8

Discussion and recommendations

Although the model gives relatively accurate results as shown in the validation, there are some minor limitations. Mostly the user interface could use some improvements, creating an understandable, well-designed layout to show to customers. Next to that, the physics is not completely researched yet, so after wind tunnel or CFD test results are available, the model could benefit from more specific interaction coefficients. The model can always be improved, examples for improvement are listed in the recommendations.

8.1. Recommendations

While there are possible improvements to the model and research, they were not included due to the scope of this thesis. The scope was defined as an early-stage placement model that considers multiple (simplified) aspects. However, time-consuming calculations and the inclusion of additional systems, such as different foundations or VentoFoil types, were not feasible within the graduation timeframe. This limitation also represents one of the model's key strengths: providing a quick estimation of the costs and benefits of VentoFoil placement on board. While the recommendations would increase the accuracy of the results, it is important to consider at what point the model could become too detailed and computationally intensive, requiring more than just the main vessel and normal operation parameters. However, if the model can handle both low and high-fidelity input in different ways, the model would become multifunctional. It could be used in early-stage decision-making and then with high-fidelity modelling be optimized. Examples for improvement include:

- The speed at reference power is calculated assuming one speed and a varying power. At the end of the process, it became clear that it would make more sense to keep the power fixed. In real scenarios, the vessel should keep a fixed power and if the wind is blowing the vessel will sail faster. The choice for the method of keeping the speed fixed was convenient for the power reduction case and was then extended for the speed increase scenario. However, for the VentoFoils at reference power, the power should be considered fixed and the speed should fluctuate depending on the wind.
- The forces on the vessel within this model are assumed to be in balance. The ship's motions are not taken into account. An improvement would be to consider the roll motion in the model to get the influence of sailing on the ship's motions and the influence of the rolling on the windspeed at the height elements of the VentoFoil, influencing the effectiveness of the VentoFoil.
- Just like the deckhouse is modelled, creating a shadow effect if VentoFoils are placed too close, it would be a useful addition to the model to place other obstructions on board. This came out of the validation of the model considering sea trials of an existing vessel with cranes on the deck, which had a significant influence on the VentoFoil performance. The cranes modelled as blocks just like the deckhouse, would improve the accuracy of the results.
- To improve the model, it would be useful to include more complex structural calculations and the possibility to select one of the other foundations. The scope of this thesis was not to focus

on the structural engineering of the foundations. Therefore, only the simplification of one of the foundations is added to the model.

- The manoeuvring capabilities of the vessel are only provided in terms of rudder angle, which remains very small. However, in reality, the added side forces have to be counteracted by the hull in some way. This could be done by adding appendages such as a bilge keel (Plessas and Papanikolaou, 2024). Moreover, these appendages could also reduce the heel angle, which is not calculated within this model. When the vessel is sailing at a significant drift angle, the Munk moment should be used to calculate the course stability of the hull. Concluding, the hydrodynamical forces acting on the vessel could be improved within the model.

At Econowind, this model will likely be adjusted to fulfil all the wishes of the sales department, since this thesis was creating a comprehensive basis of a placement model. These recommendations can be used to improve the accuracy and create the VentoFoil model that is able to handle multiple foundations and sizes of VentoFoils while remaining an early-stage tool for engineers to gain information on multiple placement options.

References

Bentin, M., Zastrau, D., Schlaak, M., Freye, D., Elsner, R., & Kotzur, S. (2016). A new routing optimization tool-influence of wind and waves on fuel consumption of ships with and without wind assisted ship propulsion systems. *Transportation Research Procedia*, *14*, 153–162.

Borren, M. (2022). The assessment of aerodynamic interaction between ventifoil suction wings: A comparison between a numerical lifting line approach and full-scale rans simulations.

Charlou, M., Babarit, A., & Gentaz, L. (2023). A new validated open-source numerical tool for the evaluation of the performance of wind-assisted ship propulsion systems. *Mechanics & Industry*, *26*, 26.

Chemship BV. (2024). *A voyage full of innovation*. Retrieved April 10, 2024, from https://www.linkedin.com/feed/update/urn:li:activity:7168652732772372481/

Chica, M., Hermann, R., & Lin, N. (2023). Adopting different wind-assisted ship propulsion technologies as fleet retrofit: An agent-based modeling approach. *Technological Forecasting and Social Change*, *192*, 122559.

Chou, T., Kosmas, V., Acciaro, M., & Renken, K. (2021). A comeback of wind power in shipping: An economic and operational review on the wind-assisted ship propulsion technology. *Sustainability*, *13*(4). https://doi.org/10.3390/su13041880

Cousteau, J., Charrier, B., Constans, J., Daïf, A., Malavard, L., & Quinio, J. (1985). Foundation cousteau and windship propulsion. *Journal of Wind Engineering and Industrial Aerodynamics*, *20*, 39–60.

de Gayffier, X. (2023). Aerodynamical investigation on the ventofoil. *Business Confidential*.

Dekking, F., Kraaikamp, C., Lopuhaä, H., & Meester, L. (2005). *A modern introduction to probability and statistics*. Springer.

Econowind. (2023). Upgrade in design: From ventifoil to ventofoil.

Econowind. (2024). Foundation nyk installation.

Gehlert, P., Cherfane, Z., Cafiero, G., & Vassilicos, J. C. (2021). Effect of multiscale endplates on wingtip vortex. *AIAA Journal*, *59*(5), 1614–1628. https://doi.org/10.2514/1.J059878

Groot, R. (2024a). *Eedi reference lines for ship types* (tech. rep.) (Internal document, Excel file). Econowind.

Groot, R. (2024b). *Tco ventofoil 16m and 30m*$_{lowestpaybackrevd}$ (tech. rep.) (Internal document, Excel file). Econowind.

Hermans, J. (2024). *Retrofit modeling for green ships* [Master's thesis, TU Delft].

HHX.Blue. (2024a). Financial model. https://hhx.blue/eu-projects/web-tools/financial-model

HHX.Blue. (2024b). Technical selection. https://hhx.blue/eu-projects/web-tools/technical-selection

Hibbeler, R. C. (2016). *Mechanics of materials* (10th). Pearson.

Hooft, J. (1994). The cross-flow drag on a manoeuvring ship. *Ocean Engineering*, *21*, 329–342.

Houbraken, M. (2018, January). *The effect of formulation on the volatilisation of plant protection products* [Doctoral dissertation, Ghent University].

Houghton, E., Carpenter, P., Collicott, S., & Valentine, D. (2017). *Aerodynamics for engineering students (seventh edition)* (7th edition).

IDL metals. (2024). *Hea steel beams*. Retrieved July 2, 2024, from https://metals.lv/en/steel-beams/hea-metal-beams/

IMO. (2009). *Second imo ghg study 2009*. Retrieved September 9, 2024, from https://wwwcdn.imo.org/localresources/en/OurWork/Environment/Documents/SecondIMOGHGStudy2009.pdf

IMO. (2021a). 2021 guidance on treatment of innovative energy efficiency technologies for calculation and verification of the attained eedi and eexi. *MEPC.1*, *896*, 1–31.

IMO. (2021b). *Annex 12 — 2021 guidelines on the operational carbon intensity reduction factors relative to reference lines*. Retrieved August 28, 2024, from https://wwwcdn.imo.org/localresources/en/OurWork/Environment/Documents/Air%20pollution/MEPC.338(76).pdf

IMO. (2024a). *Annex — unified interpretation of solas regulations ii-1/5.4 and ii-1/5.5, relating to the amendment to the stability/loading information in conjunction with the alterations of lightweight*.

Retrieved August 1, 2024, from https://www.imorules.com/GUID-77CEE06A-1A4A-4BC3-80C7-6FE7E23C9D86.html
IMO. (2024b). *Regulation 22 – navigation bridge visibility*. Retrieved August 1, 2024, from https://www.imorules.com/GUID-C61F9438-B76B-43FF-8D75-20FA41BF8C61.html
Inoue, S., Hirano, M., Kijima, K., & Takashina, J. (1981). A practical calculation method of ship maneuvering motion. *International Shipbuilding Progress*, *28*, 207–222.
Kisjes, A. (2017). *Wind propulsion for merchant vessels* [Master's thesis, TU Delft].
Klein Woud, H., & Stapersma, D. (2002). *Design of propulsion and electric power generation systems* (1st ed.). IMarEST.
Krantz, G. (2016). *Blue route*. Retrieved April 29, 2024, from https://www.egcsa.com/wp-content/uploads/CO2-and-sulphur-emissions-from-the-shipping-industry.pdf
Kühne Logistics University. (2024). Wasp decision support tool. https://www.klu.org/faculty-research/excellence-centers/hapag-lloyd-center-for-shipping-and-global-logistics-csgl/cargo-ship-calculator
Lagendijk, L. (2018a). Pooldiagrammen, EEXI & Business case.
Lagendijk, L. (2018b). Performance investigation of ventifoil ship propulsion.
Louisiana Tech University. (n.d.). Boundary layer notes [Accessed: 2024-08-05]. https://www2.latech.edu/~sajones/June/Study%20Guides/ChVIIa.pdf
Marchaj, C. (2003). *Sail performance: Techniques to maximize sail power* (Revised ed.). International Marine & McGraw-Hill.
MARIN. (2024). *Blue route*. Retrieved April 29, 2024, from https://blueroute.application.marin.nl/
Müller, M., Götting, M., Peetz, T., Vahs, M., & Wings, E. (2019). An intelligent assistance system for controlling wind-assisted ship propulsion systems. *2019 IEEE 17th International Conference on Industrial Informatics (INDIN)*, *1*, 795–802.
Pedersen, K., Emblemsvåg, J., Bailey, R., Allen, J., & Mistree, F. (2000). Validating design methods & research: The validation square. *2000 ASME Design Engineering Technical Conferences*.
Peterka, J., Meroney, R., & Kothari, K. (1985). Wind flow patterns about buildings. *Journal of Wind Engineering and Industrial Aerodynamics*, *21*, 21–38.
Plessas, T., & Papanikolaou, A. (2024). Optimization of ship design for the effect of wind propulsion. *IMDC-2024*.
Polakis, M., Zachariadis, P., & de Kat, J. (2019). The energy efficiency design index (eedi). In H. N. Psaraftis (Ed.), *Sustainable shipping: A cross-disciplinary view* (pp. 93–135). Springer International Publishing. https://doi.org/10.1007/978-3-030-04330-8_3
Prandtl, L., & Betz, A. (1932). *Ergebnisse der aerodynamischen versuchsanstalt zu göttingen; iv. lieferung*. Kaiser Wilhelm Institute for Fluid Dynamics.
Reche-Vilanova, M., Hansen, H., & Bingham, H. (2021). Performance prediction program for wind-assisted cargo ships. *Journal of Sailing Technology*, *6*, 91–117.
Simley, E., Fleming, P., Girard, N., Alloin, L., Godefroy, E., & Duc, T. (2021). *Results from a wake-steering experiment at a commercial wind plant: Investigating the wind speed dependence of wake-steering performance*. Retrieved September 9, 2024, from https://wes.copernicus.org/articles/6/1427/2021/
SWZ Maritime. (2024). Chemship fits tanker with econowind's ventofoils. https://swzmaritime.nl/news/2024/02/19/chemship-fits-tanker-with-econowinds-ventofoils/
Terntank. (2024). Safety & environment. https://terntank.com/
The Engineering ToolBox. (2004). *Drag coefficient*. Retrieved July 29, 2024, from https://www.engineeringtoolbox.com/drag-coefficient-d_627.html
The European Parliament and the Council of the European Union. (2023). Regulation on the use of renewable and low-carbon fuels in maritime transport, and amending directive 2009/16/ec. *Official Journal of the European Union*.
The Maritime Executive. (2024). Nyk with cargill to test its first wingsails on a bulker. https://www.maritime-executive.com/article/nyk-with-cargill-to-test-wingsails-on-a-bulker
Tillig, F., & Ringsberg, J. (2019). A 4 dof simulation model developed for fuel consumption prediction of ships at sea. *Ships and Offshore Structures*, *14*, 112–120.
Tillig, F., & Ringsberg, J. (2020). Design, operation and analysis of wind-assisted cargo ships. *Ocean Engineering*, *211*, 107603.

Van der Kolk, N., & Bordogna, G. (2024). *Pelican performance prediction software*. Retrieved April 5, 2024, from https://bluewaspmarine.com/software/

Vigna, V., & Figari, M. (2023). Wind-assisted ship propulsion: Matching flettner rotors with diesel engines and controllable pitch propellers. *Journal of Marine Science and Engineering*, *11*(5). https://doi.org/10.3390/jmse11051072

Wärtsilä. (2024). Rudder blade area. https://www.wartsila.com/encyclopedia/term/rudder-blade-area